PHOSPHORYLATION STATE MODULATES THE INTERACTION BETWEEN SPINOPHILIN AND NEUROFILAMENT MEDIUM

A Thesis

Submitted to the Faculty

of

Purdue University

by

Andrew C. Hiday

In Partial Fulfillment of the

Requirements for the Degree

of

Master of Science

May 2015

Purdue University

Indianapolis, Indiana

ACKNOWLEDGEMENTS

I would like to acknowledge Drs. A.J. Baucum and Mike Edler for their help and advice along the way. I would also like to acknowledge the Biology Department at IUPUI for giving me the opportunity to further my education in such a positive environment. Also, Drs. Jason Meyer and Teri Belecky-Adams for serving on my advisory committee and providing much-needed feedback and constructive criticism. Thank you to Dr. Lisa Jones and the Indiana School of Medicine Proteomics Core facility for mass spectrometry-based sequencing.

These studies were supported by NIH K01-NS073700 (AJB), Department of Biology funds (AJB and ACH), CTSI Core Pilot Grant (AJB).

TABLE OF CONTENTS

Page

Page

Page

LIST OF TABLES

LIST OF FIGURES

Figure Page

LIST OF ABBREVIATIONS

6-OHDA: 6-hydroxydopamine
Ala: Alanine
Asp: Aspartic acid (aspartate)
CAMKII: Calcium/calmodulin-dependent kinase II
Cdk5: Cyclin-dependent kinase 5
DA: Dopamine
GPCR: G protein-coupled receptor
GST: glutathione *S*-transferase
HEK: Human embryonic kidney
IF: Intermediate filament
IP: Immunoprecipitation
LTD: Long-term depression
LTP: Long-term potentiation
MSN: Medium spiny neuron
NF: Neurofilament.
NF-H: Neurofilament heavy
NF-L: Neurofilament light
NF-M: Neurofilament medium
PD: Parkinson's disease
PKA: cAMP-dependent protein kinase A
PP1: Serine/threonine protein phosphatase 1
PSD: Post-synaptic density
Ser: Serine
SpAP: Spinophilin-associated protein
Spino: Spinophilin

ABSTRACT

Hiday, Andrew C. M.S., Purdue University, May 2015. Phosphorylation State Modulates the Interaction between Neurofilament Medium and Spinophilin. Major Professor: A.J. Baucum.

A histological marker of Parkinson's disease (PD) is the loss of synapses located on striatal medium spiny neurons (MSNs) as a result of dopaminergic nigral cell depletion. The dendritic spines that give MSNs their name have a well-characterized structure and are the main regions of post-synaptic input. It has been shown that spines have altered functionality and morphology in many neurodegenerative diseases. Spine morphology, and potentially function, is dictated by an array of structural proteins and their associations with other proteins in a region dubbed the post-synaptic density (PSD). Spinophilin and neurofilament medium (NF-M) are two proteins that are enriched in the PSD and have potential implications in PD. Interestingly, preliminary data show that there is a decrease in the NF-M-spinophilin interaction in animal models of PD. Here it is shown that these two proteins interact in brain tissue and when overexpressed in a mammalian cell system. Moreover, we have begun to determine mechanisms that regulate this interaction.

It is known that there is a misregulation of protein phosphatases and kinases in many neurodegenerative diseases. Moreover, the phosphorylation state of a protein can

regulate its association with other proteins. Therefore, we hypothesize that the phosphorylation state of either protein affects the interaction between spinophilin and NF-M. Furthermore, we have conducted experiments utilizing protein phosphatases and kinases that are known to modulate the phosphorylation state of NF-M and/or spinophilin. Data show that both kinase and phosphatase activity and/or expression modulates the NF-M-spinophilin interaction in heterologous cell lines. Through the use of MS/MS analysis, we have begun to map specific phosphorylation sites that may play a role in regulating this interaction. Currently, we are elucidating the specific effects of these post-translational modifications on regulating the spinophilin-NF-M interaction. These data will enhance our knowledge of spinophilin's interactions and how these interactions are altered in neurological disorders such as PD.

CHAPTER 1. INTRODUCTION

1.1 Parkinson's Disease History and Pathology

Parkinson's disease (PD) is a progressive neurodegenerative disease that was first described nearly two centuries ago. In his essay, James Parkinson described the hallmark presentations of PD or the "shaking palsy": resting tremor, postural and gait instability, and hypokinesia (Parkinson 1817). Although Parkinson and others began describing the clinical presentations of PD in the early 19th century, it was not until the early 20th century that Friedrich Lewy first began to characterize the major histopathological markers of the disease, which was then known as paralysis agitans (Lewy 1912). We now know that these structures, commonly referred to as Lewy Bodies, contain α-synuclein aggregates that disrupt normal cell function, eventually resulting in the death of presynaptic cells (Spillantini *et al.* 1997).

PD most greatly affects the substantia nigra, leading to a loss of pigment and severe atrophy therein. When approximately 80% of these neurons have been lost, motor deficits discussed above begin to be observed (Rodriguez-Oroz *et al.* 2009). The sporadic form of the disease is most common. While the underlying mechanisms linked to this sporadic form are unclear, gene-gene interactions, environmental factors, and gene-environmental interactions play a role. Familial or genetic forms also exist. Common mutations found in familial PD include those in the *SNCA* (synuclein) and *LRRK2*

(leucine-rich repeat kinase 2) genes among others (Polymeropoulos *et al*. 1997; Lesage *et al.* 2006*)*. Typically, these mutations lead to improper protein aggregation and/or protein clearance resulting in formation of the aforementioned Lewy bodies and subsequent cell death (Gibb and Lees 1988; Spillantini *et al.* 1997).

Currently, there are several treatments for PD, none of which treat its underlying cause (loss of dopamine-releasing nigrostriatal neurons). Of these drugs, L-DOPA therapy is the oldest and most widely used. As will be discussed more in-depth below, one of the markers of PD is striatal dopamine (DA) depletion. L-DOPA is a DA precursor that can help mitigate this loss (Dauer and Przedborski 2003). In PD patients, L-DOPA is converted to DA, thereby attenuating many of the motor symptoms associated with the disease (Hornykiewicz 1974). However, long-term L-DOPA treatment is associated with debilitating side effects and waning efficacy. In human PD patients as well as non-human primates and rats, L-DOPA eventually leads to an increase in involuntary movements called dyskinesias (Pearce *et al.* 1995; Cenci *et al.* 1998). A more recent treatment of the disease includes deep-brain stimulation (DBS) of the subthalamic nucleus or the globus pallidus. In patients receiving this treatment, electrodes are implanted directly into the specific brain region where pulses are emitted at an appropriate frequency. This has proven very effective in decreasing the severity of PD motor symptoms (Kumar *et al.* 1998; Deep-Brain Stimulation for Parkinson's Disease Study Group 2001). However, both of these types of treatments, among others, only treat the symptoms of the disease. Treating the underlying causes of the disease has proven much more difficult (Shulman *et al.* 2011).

1.2 Brain Function and Parkinson's Disease

Normal brain function requires connectivity between different brain regions. This connectivity is achieved through the projection of axons from one brain region creating connections (synapses) in a second region (Sheng and Hoogenraad 2007). For instance, excitatory, glutamatergic neurons in the cortex project to, and synapse on, dendritic spines located on striatal medium spiny neurons (MSNs). Additionally, dopamine-containing neurons that reside in the substantia nigra also project to, and synapse on, these dendritic spines (Björklund and Lindvall 1975). This tripartite synapse (Figure 1; Sheng and Hoogenraad 2007) is the site of altered synaptic connectivity in PD, the second most common neurodegenerative disease. Specifically, there is a loss of nigral dopaminergic projections leading to downstream consequences in the dendritic spines of striatal MSNs (German *et al.* 1989). These downstream consequences include modulation of normal PKA signaling in these MSNs (Nishi *et al.,* (2008).

Glutamate release from the presynaptic nerve terminal activates glutamate receptors such as α-amino-3-hydroxy-5-methyl-4-isoxazolepropionic acid receptors (AMPARs) and N-methyl-D-aspartate receptors (NMDARs) on the postsynaptic dendritic spine (Hering and Sheng 2001). These dendritic spines, first described by Ramón y Cajal over a century ago, have a well-characterized structure and serve as the main site of postsynaptic input through a significant increase in overall dendrite surface area (Ramón y Cajal 1888; Gray 1959). Moreover, the relative number and morphology of spines is directly related to synaptic activity. For example, spines with a thinner, filopodial-like structure tend to correlate with decreased synaptic activity compared to spines with larger, mushroom-like shapes (Hering and Sheng 2001). Following glutamate

stimulation of postsynaptic receptors and depolarization of the postsynaptic neuron, there is an influx of calcium and other ions that serve as activators of signal transduction pathways. This occurs at the tip of the dendritic spine in a region dubbed the postsynaptic density (PSD) (Häusser *et al.* 2000). Additionally, it is believed that the overstimulation of glutamate receptors might be responsible for loss of receptor function in disorders such as PD. This phenomenon is termed excitotoxicity (Lynch and Guttmann 2001).

The PSD is enriched in multiple synaptic proteins that transduce glutamatergic signals and are responsible for normal synaptic connectivity (Figure 2; Sheng and Hoogenraad 2007). Knockout of one or more of these synaptic proteins can lead to changes in normal synaptic function and connectivity, including loss of long-term potentiation (LTP) or long-term depression (LTD), molecular correlates of learning and memory (Malenka and Bear 2004). In short, LTP serves as a sort of 'synaptic strengthening' following stimulus (Bliss and Collingridge 1993) while LTD is the selective loss of this synaptic strength (Massey and Bashir 2007). Furthermore, it has been postulated that proper conductance of LTD is necessary in spatial memory (Bear 1999).

Functional connectivity in the striatum is not only lost in PD patients, but also in animal models of PD. For instance, LTD is lost in 6-hydroxydopamine (6-OHDA)-treated rats, as 6-OHDA eliminates dopaminergic projections to the striatum (Calabresi *et al.* 1992; Ingham *et al.* 1989). Moreover, dopamine depletion in rodents, non-human primates, and human PD patients leads to decreased striatal MSN dendritic spine number, a change in dendritic spine shape, and a decrease in the overall length of the dendrites. Also seen is a rearrangement of the post-synaptic proteins found in the PSD (Ingham *et*

al. 1993; Villalba *et al.* 2009; Stephens *et al*. 2005). While the mechanisms underlying loss of dendritic spines have not been fully appreciated, calcium influx via calcium channels is suspected to play a critical role (Day *et al.* 2006). As stated above, calcium influx can activate downstream signaling cascades, which play a role in modulating spine density and/or morphology.

As noted in the previous section, one of the major causes of PD is striatal DA depletion as a consequence of nigrostriatal neuronal loss (Albin *et al.* 1989). These nigrostriatal neurons synapse on striatal MSNs. These striatal MSNs exist in two distinct populations: those that contain dopamine D_1 receptors and those that contain dopamine D_2 receptors (described below; Strange 1993). The D_1 family of receptors are $G_{\alpha S}$-protein-coupled and activate adenylyl cyclase and downstream PKA signaling. In contrast, the D_2-family of receptors are $G_{\alpha i}$-coupled and inhibit adenylyl cyclase and downstream PKA signaling (Stoof and Kebabian 1981). In normal brain function these 'direct' and 'indirect' pathways (D_1 and D_2 pathways, respectively) are balanced, resulting in the stimulation of normal movement as well as the inhibition of improper movement (Albin *et al.* 1989; Figure 3; Frank *et al.* 2004). In PD, this balance is upset, resulting in patient's difficulty conducting voluntary movements (Starr 1995).

1.3 Spinophilin Function and Localization

It has been shown that Ca^{2+} is primarily localized to the spines of hippocampal neurons (Berridge 2006), suggesting that a major function of spines is to localize calcium (Yuste *et al.* 2000). The presence of Ca^{2+} is necessary to activate signaling molecules

such as protein kinases and phosphatases (Kennedy 2000; Sheng and Kim 2002) leading to the activation of downstream processes via phosphorylation and/or dephosphorylation. Specifically, in PD there is increased phosphorylation and activation of Ca^{2+}/calmodulin-dependent protein kinase II (CaMKII) (Picconi *et al.* 2004; Brown *et al.* 2005). This increase in phosphorylation may be due to changes in the activity of the serine/threonine protein phosphatase 1 (PP1) (Brown *et al.* 2005), a highly conserved protein phosphatase that has a wide array of functions in eukaryotes (Bollen *et al.* 2010). Interestingly, phosphatase activity is highly promiscuous and is often regulated by specific interacting proteins known as regulatory subunits or targeting proteins.

Spinophilin is a recently discovered protein that was previously thought to be an integral part of PP1. In fact, it is so often found colocalized with PP1 that it was originally named 'PP1-binding protein' (Allen *et al.* 1997). Spinophilin can target PP1 to specific substrates, such as components of the neuronal cytoskeleton (Ragusa *et al.* 2010), such as F-actin (Grossman *et al.* 2004; Terry-Lorenzo *et al.* 2002) and is essential to proper spine structure and function (Allen *et al.* 1997). However, PP1 activity towards certain substrates can be inhibited when tightly bound to spinophilin (Bollen *et al.* 2010; Ragusa *et al.* 2010). Dopamine depletion leads to a decrease in PP1 activity, which might also occur in striatal neurons of human PD sufferers (Brown *et al.* 2008). Because spinophilin binds directly to the catalytic subunit of PP1, it is possible that this change of function may be due to improper targeting of the phosphatase in PD (Ragusa *et al.* 2010). Interestingly, the association of PP1 with spinophilin is enhanced in a rat model of PD (Brown *et al.* 2008).

Furthermore, it has been shown that spinophilin can associate with CaMKII and may be important in targeting the CaMKIIα isoform to F-actin (Baucum *et al.* 2012; Carmody *et al.* 2008; Terry-Lorenzo *et al.* 2005). Additionally, the interaction of spinophilin with F-actin is modulated by phosphorylation of spinophilin at the N-terminal, F-actin binding domain (Grossman *et al.* 2004; Feng *et al.* 2000; Hsieh-Wilson *et al.* 2003). It is especially important to note that the spinophilin/F-actin interaction has been shown to affect synaptic plasticity, spine maturation, and spine maintenance (Feng *et al.* 2000; Nakanishi *et al.* 1997; Zito *et al.* 2004) as actin is also enriched in dendritic spines (Cingolani and Goda 2008). This is supported by evidence suggesting that spinophilin aids in binding F-actin to the cell membrane (Satoh *et al.* 1998).

As previously noted, spinophilin has been shown to directly interact with CaMKII (Baucum *et al.* 2012) and is primarily localized within 100nm of the PSD (Muly *et al.* 2004). Given its interactions with F-actin, PP1, and CaMKII it is likely that the alterations to spinophilin and its interactions with other synaptic proteins is important in regulating normal synaptic function and spine morphology. Consistent with this hypothesis, spinophilin knockout mice show an increase in spine density at postnatal day 15 (Feng *et al.* 2000) and have altered LTD (Allen *et al.* 1997; Feng *et al.* 2000). Conversely, knockdown of spinophilin in hippocampal cultures leads to decreased dendritic spine density (Evans *et al*., 2015). Moreover, function of synaptic receptors, such as AMPARs and NMDARs, by PP1 is due to proper targeting of PP1 by spinophilin (Yan *et al.* 1999; Liu *et al.* 2006), further implicating the necessity of spinophilin in normal brain function. A more recent study utilizing spinophilin knockout mice

implicates spinophilin in G protein-coupled receptor (GPCR) sensitivity (Lu *et al.* 2010), demonstrating a role for spinophilin in G-protein signal transduction cascades.

Proteomics approaches have identified multiple spinophilin interacting proteins in mouse striatal tissue (Baucum *et al.* 2010). Interestingly, multiple intermediate neuronal filament (neurofilament) proteins were detected in spinophilin immunoprecipitations (IPs). These interactions were specific as no there were no spectral counts matching these proteins in IPs from knockout spinophilin tissue (Baucum *et al.* 2010). From these studies, it can be inferred that spinophilin interacts with multiple cytoskeletal proteins (i.e. F-actin, neurofilament medium, etc.) in MSN dendrites, potentially playing a role in spine formation and dynamics.

1.4 Intermediate Filament Function and Localization

Neurofilaments are typically comprised of four distinct intermediate filament (IF) subunits dubbed neurofilament (NF) light, medium, and heavy, (NF-L, M, and H respectively), and α-internexin. NF-L, M, and H were first described in the 1970s as the 68,000 160,000, and 210,000 Dalton polypeptides, respectively, in studies identifying large axonal proteins (Hoffmann and Lasek 1975; Schlaepfer and Freeman 1978). These proteins contain three distinct domains; head, rod, and tail and it is believed that the highly conserved rod domain is key to proper interactions between NF proteins (Yuan *et al.* 2012; Bocquet *et al,* 2009). Although NFs are mainly localized to axons, they are also present in dendrites and have demonstrated widespread effects in neurodegenerative diseases (Yuan *et al*. 2012), which will be discussed below.

Of importance, NF proteins have been proven to be important factors in dendritic arborization, implying that proper function of NF proteins is essential for synaptic connectivity (Kong *et al.* 1998). Furthermore, NFs are also major players in axonal growth, imparting the appropriate length and radius to axons (Collard *et al.* 1995). Small projections from the tail domain of NF proteins allow for proper spacing and are responsible for extending axon radial growth. It is important to note that NF-M has a greater effect on radial growth than either NF-L or NF-H (Rao *et al.* 2003). Overall, various studies have shown that the normal expression of NFs is critical to normal neuronal structure and function.

Numerous studies have examined the phosphorylation state of NFs and the effects of these modifications. In fact, early studies identified abnormal phosphorylation as the cause of structural and functional changes in NF-M and NF-H (Carden *et* al. 1984). Others have shown that an increase in expression of both NF-M and NF-H leads to disruption of dendritic arborization, and therefore synaptic connectivity (Kong *et al*. 1998). Specifically, improper accumulation or disruption of all three types of IFs are characteristic of PD as well as amyotrophic lateral sclerosis (ALS), among other neurodegenerative disorders (Al-Chalabi and Miller 2003; Julien 1999).

Additional data suggest that a high level of NF-M phosphorylation leads to its improper aggregation as well as disruption of its interaction with other cytoskeletal proteins (Al-Chalabi and Miller 2003; Gou *et al.* 1998; Trimpin *et al.* 2004). Furthermore, multiple NF-M phosphorylation sites have been identified, many of which exist in the C-terminal tail (Betts *et al.* 1997; Cleverley *et al.* 1998). Specifically, when the tail domain of NF-M is aberrantly phosphorylated, filament assembly, cross-linking,

and transport are often disrupted, resulting in the formation of the aforementioned protein aggregates. Moreover, it has also been shown that NF proteins exist mainly in an unphosphorylated state in the dendrites (Lee *et al.* 1987; Yuan *et al*. 2012) suggesting that proper dendritic function is dependent, in part, upon proper NF post-translational modifications. Interestingly, neurofilament aggregates are sometimes present in cytoplasmic inclusions commonly known as Lewy bodies, which are frequently seen in PD and other neurodegenerative diseases (Kong *et al.* 1998; Betts *et al.* 1997). In addition, polymorphisms in NF-M have also been shown to increase the risk of PD (Kruger *et al.* 2003). Together, these data demonstrate that normal NF function and its dysfunction are linked to phosphorylation state and that these proteins are altered in PD.

1.5 Neuronal Function of Protein Kinases and Phosphatases

Phosphorylation status is modulated by protein kinases and phosphatases. In eukaryotes, these enzymes are some of the most widely expressed. In fact, it is estimated that the human genome contains upwards of 500 kinases (Manning et al., 2002) and 150 phosphatases (Cohen 2002). Importantly, these proteins regulate and/or modulate a plethora of neuronal processes including synaptic plasticity, axon/dendrite formation, and others (Soderling 2000).

Phosphorylation is regulated by a balance between kinase and phosphatase activity. Therefore, regulation of kinase or phosphatase activity or localization has significant effects on its substrate phosphorylation (Cohen 1992; Meiselbach *et al.* 2006). Interestingly, there are ~385 kinases that have serine/threonine activity (Manning et al., 2002); however, there are only ~40 serine/threonine phosphatases (Cohen 2002) that

balance the activity of these kinases. In order to obtain substrate selectivity, these phosphatases associate with specific targeting or regulatory proteins (Janssens *et al.* 2008; Cohen 2002; Scott and Pawson 2009).

Protein phosphatase 1 (PP1) is a serine/threonine phosphatase that is an important regulator of synaptic receptor function. In order to obtain specificity, the PP1 catalytic subunit associates with >50 targeting or regulatory proteins (Cohen 2002), usually via an R-V-x-F-type motif (Ceulemans and Bollen, 2006; Meiselbach et al., 2006). This protein phosphatase, which is localized to dendritic spines, directly binds spinophilin and it is thought that spinophilin is responsible for PP1 targeting to downstream substrates (Allen *et al.* 1997). It is also believed that PP1 has effects in the down-regulation of AMPARs (Yan *et al.* 1999), one of the most common glutamate receptor types. This same study also shows that when PP1 and spinophilin dissociate, AMPARs become dephosphorylated, leading to decreases in channel activity. Interestingly, Yan and colleagues, among others, suggest that the effects of PP1 on AMPARs are directly reversed by a cAMP-dependent protein kinase (protein kinase A; PKA), which will be discussed below (Roche *et al.* 1996). A more recent study has also shown that spinophilin can target PP1 to additional substrates such as CaMKII, an important protein kinase. This study also demonstrated an age-dependent increase in this targeting (Baucum *et al.* 2012). It is important to note that PP1 activity is also decreased through the activation of DARPP-32, a small regulatory protein that is prominent in the CNS. This activation of DARPP-32 occurs as a result of phosphorylation via PKA (discussed below; Fienberg *et al.* 1998; Svenningsson *et al.* 2004).

PKA is highly abundant in the CNS and is one of the most important kinases in modulating glutamate receptor phosphorylation (Tingley *et al.* 1997). Previous studies suggest that phosphorylation of these receptors has effects in important neurological processes such as LTD and LTP (Raymond *et al*. 1993; Roche *et al.* 1994). Additional research has shown that PKA activation has a significant effect on neurite formation in developing cells (Weisenhorn *et al.* 2001) and can phosphorylate important structural proteins such as NF-M and NF-H (Cleverley *et al.* 1998; Sihag *et al.* 1999). Furthermore, PKA activity is modulated in rat models of PD and following long-term treatment with L-DOPA (Oh *et al.* 1997).

PKA is one of the most important second-messenger kinases and its activity can be modulated through dopamine signaling pathways as noted in section 1.2. As mentioned above, activation of D_1 receptors increases adenylyl cyclase activity (Stoof and Kebabian 1984; Sibley and Monsma 1992; Herve *et al.* 2001). Adenylyl cyclase then cleaves phosphate groups from ATP and refolds the molecule to form cAMP. cAMP then binds to the regulatory subunit of PKA allowing for the release of the active catalytic subunit (PKAc). The indirect pathway is complementary in that dopamine activation of D2-family of receptors inhibits adenylyl cyclase, resulting in inhibition of PKA (Stoof and Kebabian 1984; Sibley and Monsma 1992). It is important to remember that dopaminergic neurons synapse on striatal MSNs that also receive excitatory glutamatergic inputs. PKA is important in regulating glutamate-dependent activation of its receptors (Surmeier *et al.* 2007). Specifically, glutamate signaling is affected by the phosphorylation of glutamate receptors via PKA (Tingley *et al.* 1997).

Cyclin-dependent kinase 5 (Cdk5) is also an important neuronal protein kinase that was originally believed to have effects in the cell cycle, but this has since been disproven. Furthermore, Cdk5 is a misnomer, as it has been shown to operate independent of cyclin (Dhavan and Tsai 2001). However, it has been shown that ablation of Cdk5 expression is fatal in mice due to improper formation of the cortex. This activity is specific to tissue of the CNS, as formation of various other organs was unaffected (Ohshima *et al.* 1996). Furthermore, there is evidence that suggests Cdk5 is an important regulator of neurite growth in newly differentiated cells (Sharma *et al.* 1999). The aforementioned study by Ohshima and colleagues also suggest that improper phosphorylation of IFs by Cdk5 leads to accumulation of these proteins in cell bodies due to the disruption of axonal transport. Importantly, IF phosphorylation via Cdk5 has been demonstrated using proteins isolated from mouse and rat (Shetty *et al.* 1993). Cdk5 has also been shown to phosphorylate the important neuronal protein Tau, leading to its aggregation in Alzheimer's disease (Baumann *et al.* 1993).

Moreover, Cdk5 has dynamic affects in dopamine-signaling pathways. It has been shown that DARPP-32 inhibits PKA when phosphorylated at a Cdk5 phosphorylation site (Bibb *et al.* 1999). Cdk5 can also phosphorylate protein phosphatase inhibitor 1 which will cause the phosphatase to remain in an inactive state. This allows for the maintenance of PP1 activity and implicates Cdk5 as an indirect PKA antagonist (Bibb *et al.* 2001). Taken together, these data suggest that proper protein kinase and phosphatase activity, and a balance between the two, is necessary for proper synaptic formation, structure and function.

1.6 Hypotheses

Taken together, these data suggest that changes in the NF-M/spinophilin interactome may modulate dendritic spine morphology and/or maintenance, which could in turn alter post-synaptic signaling. Changes in neurofilament-spinophilin interactions might also have a significant impact on the overall dendritic structure. The modulation of these aforementioned interactions may have implications in a variety of neurodegenerative diseases. However, specific protein-protein interactions involving important structural proteins, such as neurofilament proteins and spinophilin, have not yet been fully characterized. It was our goal to begin elucidating these interactions beginning with the aforementioned spinophilin/NF-M interaction. Previous data (presented above; Baucum *et al.* 2010; Table 1) show that NF-M and spinophilin associate specifically in striatal lysates.

Discussed above, there are differences in phosphatase activity in animal models of PD. We have also found that both Cdk5 and PKA phosphorylation sites on spinophilin become phosphorylated in 6-OHDA lesioned animals (unpublished observations). Taken together, these data suggest that a balance of protein-protein interactions and potentially downstream kinase and phosphatase activity is essential in maintaining normal synaptic connectivity and brain function. Therefore, we hypothesized that the phosphorylation state of spinophilin regulates its interactions with the structural protein NF-M. Moreover, we hypothesize that alterations in spinophilin associations with NF-M will alter the targeting of PP1 and/or CaMKII to NF-M to regulate NF-M phosphorylation.

CHAPTER 2. MATERIALS AND METHODS

2.1 Generating DNA Constructs

2.1.1 PCR

Full-length spinophilin constructs were amplified using end-point polymerase chain reaction (PCR) using a human spinophilin template (a gift from Dr. Maria Vivo, University of Naples "Federico II"). The PCR products were ligated into a pDONR221 vector (Life Technologies, Carlsbad, CA) and subsequently Gateway-cloned into various destination vectors for protein expression (see below). For proteins intended to have a C-terminal tag when expressed, Shine-Kozak sequences were added to each forward primer. For proteins intended to have an N-terminal tag, a stop codon was added to each reverse primer. Reactions were performed using either Q5 DNA polymerase obtained from New England Biolabs (Ipswich, MA) or VAPRase DNA polymerase obtained from Vanderbilt University Medical Center (Nashville, TN). Buffers used were specific to each individual polymerase. Each reaction was given a 2 minute initial denaturation phase at 98°C. A 30 second denaturation phase at 98°C followed by a 10 second annealing phase and a 4 minute extension phase at 72°C were repeated 30 times in standard reactions. Annealing phases were run on a gradient with various ranges according to specific melting points of oligonucleotides (gradient usually ranged from 60-75°C). A final elongation phase of 12

minutes at 72°C was performed. PCR products were mixed with 6x loading dye and separated on 1% agarose gels containing SYBR Safe obtained from Life Technologies (Carlsbad, CA). Gels were typically run for ~30-40 minutes at 80-90V. The appearance of a band of the appropriate size (i.e. 2445 base pairs for full-length spinophilin) indicated that the correct sequence had been amplified. These bands were then excised from the gel and DNA was isolated using a DNA gel extraction kit (Zymo Research, Irvine, CA or ThermoFisher Scientific, Waltham, MA). DNA was typically eluted in TE or molecular biology grade deionized water and quantified using the BioTek Cytation 3 system (BioTek Instruments, Inc. Winooski, VT). Spinophilin fragments containing AA1-154, 151-301, and 1-301 were also produced using the techniques outlined above. All vectors were sequence verified (GENEWIZ, Inc., South Plainfield, NJ).

2.1.1.1 Mutagenesis PCR

Mutagenesis reactions were used in order to change either one or two nucleotides in a spinophilin sequence encoding amino acids 1-154. Primers were designed using the QuikChange site-directed mutagenesis online tool (Agilent Technologies, Santa Clara, CA). Reactions were performed using Q5 DNA polymerase along with 50 ng of template DNA. Reaction conditions included an initial denaturation of 98°C for 2 minutes. A 45 second 98°C denaturation, a 1 minute annealing, and a 15 minute elongation at 68°C were repeated 18 times before reactions were terminated. 10µL of the reaction mixtures were then digested using 1µL of dpn1 for ~2 hours at 37°C. These mixtures were stained and separated on a 1% agarose gel. If samples contained the proper banding pattern, 1 µL

of the original undigested PCR mixture was used to transform competent *E. coli*, which were cultured as below. Vectors were sequence verified (GENEWIZ, Inc.). Proteins were purified from bacteria, as outlined in section 2.2.2.

Human spinophilin (Uniprot ID: Q96SB3) amino acids 1-154 were aligned with amino acid sequences for mouse (Uniprot ID: Q6R891) and rat (Uniprot ID: O35274) using Uniprot alignment tool (http://www.uniprot.org/align/; accessed 02/27/2015) in order to determine sequence homology (Figure 20).

2.1.2 Gateway BP Cloning

Following PCR, products were recombined with donor vector (pDONR 221) using BP Gateway cloning technology from Life Technologies. 35-50 fmol of PCR product was used in each reaction with BP Clonase II enzyme mixture as well as 150 ng of plasmid vector. Reactions were performed at 25°C for 4 hours to overnight. Mixtures were then treated with proteinase K for 10 minutes at 37°C and 10 µL was used to transform DH5α competent *E. coli* from New England Biolabs. Cells were plated onto Luria broth (LB) -agar with kanamycin and incubated overnight at 37°C. Individual bacterial colonies were isolated and placed into 5mL liquid LB cultures with kanamycin and allowed to incubate overnight at 37°C.

At the end of the overnight incubation, cells were harvested and lysed. DNA was then purified from the lysate using miniprep purification kits from Zymo Research or Thermo Scientific. DNA was quantified as described above. 0.5-2 µg of the resulting DNA was digested diagnostically using appropriate restriction enzymes and separated on a 1% agarose gel before imaging on a Bio-Rad Gel Doc EZ (Bio-Rad Laboratories, Inc.

Hercules, CA). If appropriate bands were present, samples were prepared for sequencing and mailed to GENEWIZ, Inc. for analysis. Sequence verified samples were used in an additional transformation and DNA was purified from LB cultures containing kanamycin. 50-250 mL cultures were used for either midi or maxiprep purification kits from either Zymo Research or Thermo Scientific. Purified DNA was submitted to an additional restriction digest in order to confirm the presence of the appropriate insert.

2.1.3 Gateway LR Cloning

If donor vector products were found to be correct by sequencing and restriction digest, DNA inserts were then shuttled into a variety of different destination vectors for various uses. Most commonly, the pET-DEST42 and pDEST15 vectors were used for His- and GST-tagged protein expression in *E. coli,* respectively. For mammalian protein expression, pcDNA3.1 vectors with either V5, myc, or HA tags were used. Additionally, pcDNA-pDEST40 was used for expression of V5-His-tagged proteins in mammalian cells. LR reactions were performed using 150ng of template DNA (typically donor vector containing desired insert) at 25°C for 1 hour. Proteinase K digestion followed the LR reaction at 37°C for 10 minutes. Competent DH5α *E. coli* were transformed using 1-5 µL of the reaction mixture and grown on LB plates in the presence of ampicillin at 37°C.

Bacterial colonies were plucked after overnight growth and grown in 5mL liquid LB cultures with ampicillin for an additional night. DNA was extracted as described above and screened via restriction digest. If appropriate DNA banding patterns were present, purified DNA was used to transform additional cells. These cells were used in larger (50-250 mL) cultures for either midi or maxipreps from Zymo Research or Thermo

Scientific. DNA was again screened via restriction digestion. All original empty DNA vectors used in BP or LR cloning were obtained from Life Technologies.

2.2 Bacterial Protein Expression

2.2.1 Cell Culture

Following restriction verification, competent Rosetta pLysS or BL21 cells were transformed using up to 1 µL of purified DNA. Bacteria were grown on LB agar plates overnight in the presence of ampicillin. Individual bacterial colonies were isolated after overnight incubation and placed into 5mL LB cultures for approximately 8 hours to overnight. 5 mL cultures were then poured into 250-500mL aliquots of liquid LB with ampicillin at 37°C. After ~2 hours of incubation, optical density levels were measured at an absorbance of 600nm (OD_{600}). Once OD_{600} levels reached ~0.6 - 0.8, 1 M isopropyl β-D-1-thiogalactopyranoside (IPTG; Life Technologies Carlsbad, CA) was added to the culture (1 mL/L) in order to induce protein expression. Bacteria were induced and cultured at 37°C for ~4 hours or at 16°C overnight.

2.2.2 Glutathione *S*-transferase-tagged Protein Purification

Bacteria were pelleted at 4000 x g for 20 minutes and resuspended in lysis buffer (50 mM Tris-HCl pH 7.5, 100 mM NaCl, 0.5 mM PMSF, 1 mM benzamidine, 5 mM EDTA, 0.5% Triton X-100, 1.0 g/L lysosome, 0.5x protease inhibitor cocktail). Bacterial suspensions were sonicated (30 second pulse, 55 second rest at 40% amplitude eight times; Model 505 Sonic Dismembrator, Thermo Fisher Scientific, Waltham, MA) at 4°C

and centrifuged (12000 x g for 25 minutes at 4°C). The resulting supernatant was then incubated with glutathione agarose beads previously washed in lysis buffer for ~1h at 4°C. Beads were collected on a filter column and washed multiple times in wash buffer (50 mM Tris-HCl pH7.5, 200 mM NaCl, 50 µM PMSF, 0.1 mM benzamidine, 0.1 mM EDTA, 0.5% Triton X-100) before proteins were eluted in 3mL 20mM glutathione (pH 8.0). Eluate was placed into Slide-A-Lyzer cassettes and dialyzed in storage buffer (10 mM HEPES pH 7.5, 25 µM PMSF, 62.5 µM benzamidine, 62.5 µM EDTA, 0.1% Triton X-100) for two hours with rotation at 4°C. Storage buffer was then exchanged and samples were dialyzed overnight at 4°C. Finally, the eluate was removed from the cassettes via syringe and proteins were quantified using the Cytation 3. For quantifications, 5 µL of purified protein was added to 2mL Bradford reagent (Bio-Rad Laboratories, Hercules, CA) in a cuvette. Samples were incubated at room temperature for ~5 minutes. Raw data was quantified using GraphPad Prism. Samples were stored at -80°C for long-term storage or at -20°C for more immediate use.

2.3 Mammalian Protein Expression

For mammalian protein expression, human embryonic kidney (HEK293) or mouse Neuro2a cells were used. Cells were stored long-term in liquid nitrogen and thawed at 37°C when needed. Neuro2a cells were incubated with Eagle's minimum essential medium (EMEM). HEK293 cells were incubated in Dulbecco's modified Eagle's medium (DMEM). Both media contained 10% FBS, L-glutamine, and penicillin/streptomycin. 50mm Corning or Nunc culture flasks were incubated at a constant 37°C and 5% CO_2 (Panasonic Healthcare; Secaucus, NJ).

Cells were counted and approximately 250,000 cells were plated into 25 mm flat-bottomed culture flasks and grown overnight. Cells were transfected at ~60-80% confluence. Confluence was measured by examining the approximate cell coverage on the bottom of the flask. Typically, 2 µg of each DNA was used in each transfection. The appropriate volume of DNA was added to 250 µL of serum-free medium in a 1.7mL microcentrifuge tube. In a separate tube, Lipofectamine (Life Technologies) or PolyJet reagent (SignaGen Laboratories Rockville, MD) was added to an additional 250 µL of medium. Lipofectamine was added in a 3:1 volume:mass ratio (e.g. 18 µL of Lipofectamine was used alongside 6 µg DNA). All transfections were performed using equal masses of DNA. If necessary, an empty DNA vector was used to normalize DNA concentrations across conditions. The two mixtures were then placed in a third tube and incubated at room temperature for 15-20 minutes. The entire mixture was then added to the appropriate flask and cells were incubated overnight.

After overnight growth, cells were examined to ensure adherence to flask bottoms. If there was little to no disruption of adherence of the cells, the medium was aspirated and cells were washed with 8mL cold phosphate-buffered saline (PBS). The wash was aspirated and cells were resuspended in 2 mL low ionic Tris-HCl pH 7.4 buffer + Triton X-100 buffer before transfer into 2 mL microcentrifuge tubes. If a large number of cells had become unattached, they were resuspended in medium and transferred to 15 mL centrifuged tubes and centrifuged at 250 x g for 5 minutes. Medium was aspirated and cold PBS was used to wash the cells before an additional centrifugation. PBS was then aspirated and cells were resuspended in low ionic Tris HCl buffer + Triton X-100 lysis buffer (10 mM DTT, 5 mM EDTA, 2 mM Tris-HCl pH 7.5, 1% (v/v) Triton X-100, 20

mM NaF, 20 mM β-glycerophosphate, 20 mM $NaVO_3$, 10 mM Na pyrophosphate, 1% Halt protease inhibitor cocktail; Thermo Scientific Waltham, MA). Cells were sonicated at 4°C for 15 seconds at a 25% amplitude and centrifuged (4°C for 10 minutes at 14,000 x g). Cell lysates were then used in glutathione *S*-transferase (GST) pulldowns or immunoprecipitations as described in the following sections.

2.4 Tissue Homogenization

Male or female, WT, C57Bl6 mouse brains were dissected. Forebrain or striatal tissue was flash-frozen in liquid nitrogen and stored at -80°C for later use. Tissue was homogenized in 2mL of either low ionic Tris-HCl or isotonic KCl buffer containing 1% Triton X-100 buffer using twenty up-and-down movements of a pestle in a 2 mL tight-fitting glass homogenizer. Tissue was then transferred to a 2 mL microcentrifuge tube and processed in the same manner as HEK293 cells described above. Striatal tissue remained in 2 mL total volume of buffer while cortical tissue was brought up to 5 mL using the appropriate buffer. IPs or GST pulldowns were then performed as described below.

2.5 Immunoprecipitations

400µL of HEK293 cell lysate or brain homogenate was transferred to a 1.7 mL tube and incubated with the appropriate primary antibody at 4°C for approximately 1 hour with rotation. Primary antibodies used for immunoprecipitations were a goat polyclonal anti-HA tag (A190-107A, Bethyl Laboratories, Inc. Montgomery, TX) or goat polyclonal anti-V5 tag (A190-119A, Bethyl Laboratories, Inc.) Additionally, 75 µL of

each sample was collected to serve as a non-immunoprecipitated input. 25µL of 4X sample buffer (40% glycerol, 0.2 M Tris HCl pH 6.8, 8% SDS w/v, 0.1 M DTT, 0.04% bromophenol blue w/v in water) was added to each input and stored at -20°C. At the end of the 1-hour incubation, 30 µL of protein G magnetic beads was added to each sample. Incubation with protein G beads continued overnight at 4°C with rotation.

Protein G beads were magnetically separated and washed three times with immunoprecipitation buffer (150 mM NaCl, 50 mM Tris HCl, 0.5% Triton X-100). 80 µL of 2x sample buffer (4x buffer diluted 1:2 with Milli-Q water) was added to each of the samples.

2.6 GST Pulldowns

GST pulldowns were performed using 5µg purified GST-tagged protein. Proteins were incubated with 400µL HEK293 cell lysate, homogenized brain lysate, or 5 µg of non-GST tagged, purified protein. Total volumes were brought up to 500 µL with GST pulldown buffer (200 mM NaCl, 50 mM Tris, 0.5% Triton X-100 in water). Samples were incubated for 1 hour at 4°C with rotation. 75 µL of each sample was collected to serve as an input, 25 µL 4X sample buffer was added to each input and stored at -20°C. 30 µL of pre-washed glutathione agarose beads (Thermo Scientific) was then added to each sample and incubated overnight at 4°C. After overnight incubation, samples were centrifuged at 2000 x g for 1 minute to pellet glutathione agarose beads and any bound proteins. The supernatant was aspirated and discarded. Beads were washed three times with GST pulldown buffer aspirating the buffer each time. 80 µL of 2X sample buffer

was added to each sample and mixed gently by inversion. Samples were heated at 70ºC for 10 minutes for SDS-PAGE and western blot analysis (see below).

2.7 SDS-PAGE and Western Blotting

Western blots were performed using samples obtained from GST pulldown or IP assays described above. IP samples were placed on a magnet before sample loading in order to pull magnetic beads out of suspension. Glutathione agarose beads were pelleted through centrifugation at 2000 x g for 1 minute before sample loading. 10 µL of each input along with 20 µL of each sample was loaded onto either a 1.0 mm or 1.5 mm hand-cast 10% polyacrylamide gels or onto a 26-well, pre-cast Criterion 4-15% or 4-20% gradient gel (Bio-Rad). Gels were typically run at 75 V for 15 minutes and 175 V for approximately 1 hour or until sample buffer dye front had run off of the gel. Proteins were then transferred to nitrocellulose membranes using one of two methods.

For high molecular weight protein analysis (over ~100kD), a wet transfer was used. Gels were placed inside a sandwich containing two rectangular filter papers as well as the nitrocellulose membrane. The sandwiches were placed into a transfer unit containing N-cyclohexyl-3-aminopropanesulfonic acid (CAPS) transfer buffer (10% MeOH, 0.01 M CAPS pH 11). The transfer unit was attached to a water chilling unit set to 2.5-4°C. Protein transfers were run at a constant 1.0 A for 90 minutes.

For proteins with low molecular weights (below ~100kD), the Bio-Rad Trans-Blot Turbo was used. Filter paper stacks and pre-cut membranes were equilibrated in cold transfer buffer for 3-5 minutes. Excess buffer was poured off and stacks were placed in a

transfer cassette with membrane beneath the gel. Transfer stacks were then rolled in order to remove excess bubbles. Transfers were then run at a constant 1.3 A for 30 minutes.

After transferring, membranes were trimmed and placed in incubation boxes. An optional Ponceau stain was often used to visualize protein transfer. Membranes were then washed with deionized water and scanned. Membranes were then blocked using 5% (w/v) nonfat dry milk in 0.1% (v/v) Tween 20 in 1 M tris-buffered saline pH 7.5 (TBST). Blocking was done 3x for 10-20 minutes. The final blocking solution was discarded and the membranes were incubated with primary antibodies (1:2000 dilution in 5% milk) overnight at 4°C with shaking. Primary antibodies used were: a goat polyclonal anti-neurabin-II (sc-14774; Santa Cruz Biotechnology, Inc. Dallas, TX), a mouse monoclonal anti-NF-M (#2838 Cell Signaling, Danvers, MA), a goat polyclonal anti-PP1γ (sc-6108 Santa Cruz Biotechnology), a mouse monoclonal anti-PKA C-α (#5842 Cell Signaling), or a goat polyclonal anti-GST (A190-121A Bethyl Laboratories, Inc.). Excess antibody was then discarded and membranes were washed 3-5 times with 5% milk for 5-10 minutes each wash. Appropriate secondary antibodies were conjugated to alexafluor 680 or 790 nm (1:10000 dilution in 5% milk) for approximately 45-60 minutes at room temperature in darkness with shaking. Secondary antibodies were discarded and membranes were washed three times with 0.1% TBST for 5-10 minutes and two times in TBS for 5-10 minutes. Fluorescence scans were obtained using the Li-Cor Odyssey and data were analyzed using Image Studio software (LiCor). Relative quantifications were calculated based on total amount of GST protein present in each sample.

2.8 Pro-Q Diamond in-gel Staining

Following SDS-PAGE, gels were stained for phosphorylated proteins. Gels were fixed using 50% MeOH/10% acetic acid in water twice for thirty minutes. Fixative was then removed and gels were washed three times for ~10 minutes with deionized water. Pro-Q Diamond staining solution from Invitrogen (ThermoFisher Scientific, Waltham, MA) was then added and incubated for ~60 minutes. Stain was removed and gels were de-stained with 20% acetonitrile, 50 mM sodium acetate in water pH 4 three times for ~30 minutes each. Finally gels were washed twice for ~5 minutes with deionized water and visualized using the Bio-Rad Gel Doc.

2.9 *In-vitro* Kinase Activation

To activate endogenous PKA in HEK293 cells, 5 mM 3-isobutyl-1-methylxanthine (IBMX) and 500 µM forskolin in DMSO were used. Cells were transfected as described above and incubated overnight. Medium was removed and replaced with DMEM containing IBMX and forskolin (1:1000 dilution). Cells were then incubated for 30 minutes to overnight at 37°C. At the end of incubation, flasks were immediately placed on ice and cells were processed as described above.

2.10 *In-vitro* Protein Phosphorylation

Active PKA (New England Biolabs, Ipswich, MA) was used to phosphorylate purified proteins *in vitro*. 50 nM PKA was used in solution with 1x NEBuffer (New England Biolabs), and 0.2 mM ATP. Volumes of GST-fused proteins were added to each reaction mixture to yield a 2 µM purified protein concentration in a total volume of 50 µL

(Q.S. with molecular biology-grade water). Separate reaction mixtures with 30mM EDTA without ATP were created to serve as mock phosphorylation controls. Reactions were incubated at 30°C for 20 minutes. 3 µL of 0.5 M EDTA was added to each mixture after incubation in order to halt kinase activity. 50 µL of each reaction mixture was incubated with 400µL of brain tissue or HEK cell homogenate along with 50 µL of GST pulldown buffer. GST pulldowns were then completed as described in section 2.5. Additionally, 5 µg His-tagged NF-M was similarly phosphorylated via PKA *in vitro* and incubated with homogenized brain lysate as described above. Pulldowns were performed using Talon resin beads via the process described in section 2.5 and immunoblotted as described in section 2.7.

2.11 Mass Spectrometry

Samples separated by SDS-PAGE were digested with trypsin and analyzed by mass spectrometry. Specifically, samples were processed at the Vanderbilt University Mass Spectrometry Research Center, in the Indiana School of Medicine Core Facility, or in the laboratory of Dr. Lisa Jones, using an LTQ Orbitrap Velos, Velos Pro, or QExactive mass spectrometer (Thermo Fisher Scientific Waltham, MA), respectively. Raw data files were converted to MzXML files using MassMatrix Mass Spec Data File Conversion Tool (Xu and Freitas, 2009). MzXML files were searched against the NCBI Reference Sequence human or mouse database using MS-GF+ (Kim *et al.,* 2010) or against the Uniprot database using MyriMatch (Tabb *et al.,* 2007). Searched files were assembled in either Scaffold 4 (Proteome Software, Portland, OR) or IDPicker (Holman *et al*., 2012). Spectral counts matching spinophilin-associated proteins were derived from these

assembled files. Tryptic fragments containing phosphorylated sites were further evaluated by measuring the area under the curve (AUC) of the extracted ion chromatogram (XIC) that matched a specific phospho-peptide. These areas were normalized to either the non-phosphorylated peptide or to a control peptide to generate a ratio of phosphorylation. These ratios were compared across different groups, as previously described (Baucum *et al.*, 2015).

2.12 Statistical Analyses

Western blots from immunoprecipitations were quantified using Image Studio software. Integrated densities for the co-immunoprecipitating protein were divided by the integrated density in the corresponding input and of the corresponding immunoprecipitated protein. All values obtained from Western blots are presented in relative units. Western blots from GST pulldowns were quantified by dividing the integrated density of the associated protein by the integrated density of the corresponding GST protein. For statistical analyses, values were normalized to a control group and compared using an unpaired *t* test (two groups) or one-way ANOVA (more than two groups).

CHAPTER 3. RESULTS

3.1 Validation of the Interaction between Spinophilin and Neurofilament Medium

Recent mass-spectrometry-based data have shown that spinophilin and NF-M co-immunoprecipitate from striatal lysates (Baucum *et al.* 2010). To further examine and validate this interaction, we immunoprecipitated spinophilin and NF-M from cortical lysates of C57Bl/6 mice. Tissue was homogenized in a Triton X-100 and KCl-containing buffer with protease and phosphatase inhibitors (see methods) in order to maintain an isotonic condition and prevent protein degradation and dephosphorylation. Western blots of NF-M and spinophilin immunoprecipitations from cortical tissue demonstrate reciprocal association between NF-M and spinophilin (Fig. 4). Reciprocal immunoprecipitations also produce these results in striatal tissue (not shown). Furthermore, immunoprecipitations using an anti-PP1 antibody isolated both NF-M and spinophilin, suggesting that all three proteins may exist in the same complex (Fig. 4). This interaction was specific as a control IgG did not precipitate spinophilin, NF-M, or PP1.

3.2 Neurofilament Medium Interacts with Spinophilin Residues 1-154 and 1-301

In order to determine the spinophilin motif that interacts most strongly with NF-M, GST pulldowns in brain homogenate as well as cell lysates from HEK293 cells were

utilized. Brain homogenates were incubated with GST-fused spinophilin fragments containing amino acids 1-154, 151-301, or 1-301 as the neurofilament protein, NF-L, has been previously shown to interact with the N-terminus of spinophilin (Baucum *et al.* 2012). Samples were submitted to SDS-PAGE and Western blots were performed using an antibody for NF-M. Qualitative data show strong NF-M pulldown when incubated with fragments containing AA 1-154 and 1-301 (Fig. 5). Similar pulldowns were also performed from HEK293 cell lysates wherein a V5-tagged NF-M was overexpressed. Qualitative data from these experiments support the observation that NF-M binds to spinophilin fragments containing AA1-154 and AA1-301 (data not shown).

3.3 PP1 Increases the Interaction between Spinophilin and Neurofilament Medium

To further validate the association of spinophilin and NF-M, we utilized a heterologous cell system, HEK293 cells, to overexpress spinophilin and NF-M. HEK293 cells overexpressing NF-M (V5-tagged) and spinophilin (HA tagged) were separated by SDS-PAGE and immnoblotted for NF-M and spinophilin. Consistent with results in tissue lysates, both proteins co-immunoprecipitated in HEK293 cells (Fig. 6A). Given that PP1 co-immunoprecipitates with spinophilin and NF-M in cortical lysates, we wanted to further validate that these proteins also interact in HEK293 cells. Moreover, previous data generated in the lab suggest that spinophilin phosphorylation and association with NF-M are increased and decreased, respectively, in an animal model of PD (Fig. 18). Therefore, we wanted to determine if PP1 activity modulates the association of these two proteins. We expressed a GFP-tagged PP1 (Carmody *et al.* 2008) in the presence of spinophilin and/or NF-M. Reciprocal IPs were performed using

antibodies for either the HA or the V5 protein tag and were analyzed by Western blot. Results revealed that addition of PP1 enhanced the association of NF-M and spinophilin by approximately 2-fold (Fig. 6B). This increased association may be due to a molecule of spinophilin and a molecule of NF-M binding the same catalytic subunit of PP1. However, it has been previously shown that PP1 does not directly bind to NF-M. However, it can bind to NF-L (Terry-Lorenzo *et al.* 2000). This is consistent with the fact that NF-M IPs contain PP1 (Fig 6A) even in the absence of spinophilin. Moreover, NF-L binding of PP1 may target spinophilin to the neurofilament complex; however, this is unlikely given many PP1-binding proteins associate via the same R-V-X-F motif (Egloff *et al.* 1997). Therefore, an alternative hypothesis is that overexpression of PP1 decreases phosphorylation of spinophilin and/or NF-M and that this phosphorylation may modulate the association. To further test this, we evaluated the effect of phosphorylation on modulating the spinophilin/NF-M interaction (discussed below).

3.4 PKA Phosphorylates Spinophilin and NF-M

Both spinophilin and NF-M are phosphorylated by multiple kinases (See introduction). Consistent with these data, in-gel phosphorylation-specific protein staining (Pro-Q Diamond) shows an increase in spinophilin (Fig 7A) and NF-M (data not shown) phosphorylation when both V5-tagged NF-M and HA-tagged spinophilin were transfected in the presence of overexpressed PKA (Fig. 7A). Pro-Q Diamond-stained gels were stained using Imperial Protein Stain. Appropriate bands were excised from the gel and sent for MS/MS analysis (Fig. 7B). Preliminary MS/MS data are consistent with the ProQ staining, showing increased phosphorylation of spinophilin and NF-M. Specifically,

spinophilin phosphorylation was increased at Ser100, Ser116, Ser126, and Ser203 (Fig 7C) and NF-M phosphorylation was increased at Ser346 and Ser736 (Fig 7D).

3.5 PKA and Phosphorylation-Dependent Modulation of the Interaction between Spinophilin and Neurofilament Medium

3.5.1 *In Vitro* Phosphorylation of Spinophilin Fragments Decreases Association with Multiple Proteins, Including NF-M.

Spinophilin fragments containing AA1-154 and AA1-301 were incubated with the purified catalytic subunit of PKA (PKAc) in the presence or absence of ATP (phosphorylated and mock samples, respectively). GST alone was used as a control. EDTA was then used to halt catalytic activity at the end of the incubation period. Mock-treated or autophosphorylated fragments were incubated with mouse cortical lysate and precipitated by glutathione agarose, separated by SDS-PAGE, and either Coomassie stained or immunoblotted for NF-M.

Interestingly, mock treated samples show a strong, non-significant increase in NF-M levels when compared to purified protein controls. This pattern is seen in samples containing spinophilin AA1-154 as well as 1-301 (Fig. 8A). However, when PKAc is active, NF-M signal returns to control levels. Despite consistency in these patterns, they contain a high level of variability (Fig. 8B; 8C). In addition to associations with NF-M, spinophilin phosphorylation by PKA decreased the intensity (Imperial stain) of many spinophilin-associated proteins (SpAPs) isolated from spinophilin GST-pulldowns using N-terminal spinophilin fragments (Fig. 9). These samples were extracted and analyzed by

MS/MS. These data reveal that spectral counts matching NF-M were lower in the phosphorylated compared to non-phosphorylated forms (Table 2).

Conversely, full-length His-tagged NF-M was phosphorylated *in vitro* via PKA and incubated with homogenized brain lysate. Talon resin beads were used to bind and pull His-tagged proteins out of suspension. Samples were then separated via SDS-PAGE and immunoblotted for spinophilin. Data reveal that PKAc, *per se*, enhanced the association of spinophilin and NF-M in the absence of ATP. There is a slightly weaker increase in samples where ATP is present. These patterns are consistent but non-significant, as there is a high level of variability (Fig. 10B).

3.5.2 Point Mutations in Spinophilin Fragments Decrease NF-M in Spinophilin Pulldowns

In order to determine the role of specific phosphorylation sites on spinophilin in modulating its association with NF-M, GST-tagged spinophilin constructs containing amino acids 1-154 containing point mutations at serine 17 and/or 100 were created. Specifically, serines were mutated to either an aspartic acid (to mimic phosphorylation) or alanine (to prevent phosphorylation). These sites were selected due to Ser17 and Ser100 being hyper-phosphorylated in a mouse model of PD (Fig. 11). Additionally, both residues were mutated to either alanine or aspartic acid. GST alone, WT or mutant spinophilin fragments containing amino acids 1-154 were incubated with cortical tissue homogenized in KCl-containing buffer. Both individual single point mutants and a double alanine mutant were highly variable (individual experiments might show either an increase in association or a decrease in association; data not shown). However, mutating

both Ser17 and Ser100 to aspartic acid consistently and significantly decreased the amount of NF-M in the spinophilin pulldowns (Fig. 12).

Sequence alignment revealed that residues Ser17 and Ser100 are conserved among human, rat, and mouse spinophilin sequences. Furthermore, amino acids 1-154 show a high level of sequence similarity among all three species (Fig. 13).

3.5.3 Short-term Activation of Endogenous PKA Attenuates the Interaction between Spinophilin and NF-M

IBMX and forskolin were used to pharmacologically activate endogenously expressed PKA in HEK293 cells. V5-tagged NF-M and HA-tagged spinophilin were transfected alone or together and cells were incubated with IBMX/forskolin in DMSO to activate PKA or in DMSO alone. Samples were immunoprecipitated for either HA or V5 and Western blots for NF-M and spinophilin were performed (Fig. 14A). Quantified data show a significant decrease in levels of NF-M in HA IPs as well as a decrease in levels of spinophilin in V5 IPs when normalized to non-immunoprecipitated inputs (Fig. 14B). Appropriate bands were excised and prepared for MS/MS analysis (Fig. 15). Preliminary data suggest that there is no difference in the levels of spinophilin phosphorylation upon short-term activation. However, phosphorylation of NF-M increases at several sites. Specifically, Ser736 and Ser837 have an ~1.5 fold increase or greater in PKA-dependent phosphorylation. NF-M has multiple repeat sequences that are phosphorylated. Specifically, Ser620 and Ser685 are on indistinguishable fragments following tryptic digestion. Interestingly, this tryptic fragment as well as a tryptic fragment phosphorylated at Ser615 and Ser620 had a 2-3-fold increase in phosphorylation. Moreover, a second

repeat sequence (with phosphorylation sites at Ser633, Ser646, and Ser659) also had PKA-dependent increases in phosphorylation. Moreover, the doubly phosphorylated peptide (with phosphorylation at Ser628 and Ser633, Ser641 and Ser646, and/or Ser654 and Ser659) was also increased by short-term PKA activation. Interestingly, when spinophilin is overexpressed with NF-M in samples where PKA has been activated, phosphorylation was attenuated all of these increases in phosphorylation (Fig. 16). These studies are currently being validated.

3.5.4 Long-Term Activation of Endogenous PKA in HEK293 Cells Enhances the Interaction between NF-M and Spinophilin

In addition to short-term activation experiments, IBMX and forskolin were used to activate endogenous PKA in HEK293 cells over a period of 16-20 hours. Cells were transfected and treated as in section 3.5.1. Surprisingly, there was a slight but significant increase in the level of spinophilin in NF-M IPs (Fig. 17). Gels were also Imperial stained and bands were excised for MS/MS analysis (Fig. 18). These data also reveal that the level of spinophilin phosphorylation is unchanged. We also analyzed levels of NF-M phosphorylation in the presence or absence of spinophilin following overnight PKA activation. Preliminary results suggest that overnight activation increased phosphorylation ~2-fold at the Ser620/685 site. Interestingly, this increased phosphorylation was attenuated by co-expression of spinophilin (Fig 19). Additional sites are also shown with variable phosphorylation. It is important to note that MS/MS data presented herein were produced from single experiments. Further replicates will need to be conducted in the future.

3.5.5 Overexpression of PKA in HEK293 Cells Increases NF-M in Spinophilin IPs

Given that purified, inactive PKA enhanced the association of spinophilin with NF-M in the GST pull-down studies and that long-term activation of PKA resulted in a slight, but significant increase in the spinophilin/NF-M interaction, we wanted to determine the effect of overexpressing PKAc on modulating the spinophilin/NF-M association in a heterologous cell system. V5-tagged NF-M and HA-tagged spinophilin were co-expressed in HEK293 cells alone or alongside myc-tagged PKA. Lysates were immunoprecipitated for either the HA (spinophilin) or the V5 (NF-M) tag. IPs were blotted for NF-M or spinophilin. Qualitatively, there was a robust increase in the association between spinophilin and NF-M in the presence of PKA (Fig. 20A). When analyzed quantitatively, this increase is shown to be approximately 20-fold (Fig. 20B). Western blots performed using an antibody for PKA also indicate that the kinase co-immunoprecipitates with both spinophilin and NF-M (Fig. 20A).

CHAPTER 4. DISCUSSION

4.1 Spinophilin Interacts with NF-M

Data previously produced have shown a specific interaction between spinophilin and NF-M in mouse brain homogenate when spinophilin knockout and wild type tissues are analyzed via MS/MS (Baucum *et al*. 2010). Here, we immunoprecipitated spinophilin or NF-M from brain lysates or transfected HEK293 cells. In order to maintain an isotonic environment similar to conditions in the brain, brain lysate experiments were performed using an isotonic KCl-containing buffer. We found that both NF-M and PP1 co-immunoprecipitate with spinophilin. Moreover, spinophilin and NF-M co-immunoprecipitate with PP1. Interestingly, NF-M IPs do not consistently precipitate spinophilin. This may be due to the NF-M antibody binding the same motif as spinophilin, higher background associated with the NF-M antibody, or differences in the stoichiometries of associations. For instance, spinophilin binding to a single NF-M molecule may pull down multiple NF-M monomers, whereas NF-M binding to spinophilin would be predicted to pull down at most two homomeric spinophilin molecules. As spinophilin has already been shown to specifically interact with PP1 (Grossman *et al.* 2004; Terry-Lorenzo *et al.* 2002), PP1 may bridge the apparent interaction between spinophilin and NF-M, as opposed to a direct interaction between

these two proteins. However, this is not likely given that PP1 tends to bind at an R-V-x-F motif in a single regulatory subunit (Egloff *et al.* 1997). Furthermore, it has been shown that NF-M and PP1 do not directly interact (Terry-Lorenzo *et al.* 2000), further suggesting that spinophilin may target PP1 to NF-M. In addition to spinophilin, NF-L binds to PP1 and may target it to NF-M. Consistent with this, PP1 co-precipitated with NF-M in transfected HEK293 cells even in the absence of overexpressed spinophilin. This may be due to NF-L binding both PP1 and NF-M. However, spinophilin and NF-L may target PP1 to different phosphorylation sites on NF-M. Future studies will need to determine functional differences between spinophilin and NF-L targeting of PP1 to NF-M.

Additional pull-down assays have been used in order to further elucidate the nature of the interaction between NF-M and spinophilin. NF-L was previously shown to pull-down with the N-terminus of spinophilin (Baucum *et al.* 2012). This finding prompted the production of spinophilin fragments containing amino acids 1-154, 151-301, and 1-301 containing a GST tag to determine if a similar region associated with NF-M. Brain tissue was again homogenized in KCl-containing buffer and incubated with these GST-fused proteins. Samples were then incubated with glutathione agarose beads, which binds to GST and can be easily removed from suspension through centrifugation (Guan and Dixon 1991). Samples were submitted to SDS-PAGE and western blots were performed using antibodies for NF-M and GST. Data were normalized to the amount of GST-fused protein (spinophilin). Results reveal that NF-M binds strongly to both the AA1-154 and binds very poorly to the fragment containing AA151-301. Also, NF-M associates with these same two fragments when V5-tagged NF-M was transfected into HEK293 cells.

Taken together, these data demonstrate specific association between the N-terminal region of spinophilin and NF-M in multiple systems and under various conditions.

4.2 PP1 Enhances the Interaction between NF-M and Spinophilin

In order to determine the effects of PP1 on the interaction between spinophilin and NF-M, overexpression experiments in HEK293 cells were performed. Spinophilin and NF-M were expressed with HA and V5 tags as above, respectively in the presence or absence of GFP-fused PP1. Spinophilin has been previously shown to target PP1 to specific substrates (Ragusa *et al.* 2010; Allen *et al.* 1997). Furthermore, 6-OHDA lesioned mice show an increase in spinophilin phosphorylation along with a decrease in the association between NF-M and spinophilin. Therefore, we hypothesized that enhanced phosphorylation may contribute to this decreased association and that overexpressing a phosphatase would enhance the interaction between spinophilin and NF-M. As expected, there is an increase in the levels of NF-M in spinophilin IPs where PP1 has also been overexpressed. As mentioned above, NF-L and spinophilin may both be targeting PP1 to NF-M. Moreover, they may modulate different sites. Interestingly, this targeting may be important in maintaining the typically low levels of basal NF-M phosphorylation (Lee *et al.* 1987; Yuan *et al*. 2012). From these results, we infer that NF-M and spinophilin naturally interact in mouse neuronal tissue. However, the nature of this interaction (i.e. direct interaction of spinophilin and NF-M, or the association of protein(s) that can bridge this interaction) is not entirely clear. However given that PP1 and NF-M do not directly interact (Terry-Lorenzo *et al.* 2000) and that it is unlikely that PP1 would be bridging an interaction, it is unlikely that PP1 is responsible for directly

bridging these proteins. We predict that PP1 is acting to decrease the phosphorylation status of spinophilin and/or NF-M and lower levels of phosphorylation are linked to an increase in the association of these proteins.

The phosphatase/kinase balance has proven necessary for many essential cellular functions, including cell division (Meraldi and Nigg 2001). More specifically, it is critical in keeping phosphorylation levels of NF-M low (Roche *et al.* 1996). In a rat model of PD there is an increase in the association with spinophilin and PP1 (Brown *et al.* 2008). This may lead to improper targeting or loss of phosphatase function (Bollen *et al.* 2010; Ragusa *et al.* 2010). Improper phosphatase function may result in downstream consequences, such as protein aggregation or altered cellular structure. Given that dendritically-localized NFs normally have low phosphorylation levels (Yuan *et al*. 2012), mechanisms that modulate NF phosphorylation may lead to improper NF localization and/or aggregation. Taken together, our data demonstrate a PP1-dependent modulation of the spinophilin/NF-M interaction and suggest that phosphorylation status is a critical regulator of the spinophilin/NF-M association. Alterations in this association may allow for regulation of PP1 targeting to NF-M by spinophilin. Future studies need to address the functional effects of this altered targeting.

4.3 PKA Activation Affects the Interaction between NF-M and Spinophilin

Given our hypothesis that phosphorylation *per se* modulates the spinophilin/NF-M association and that overexpression of PP1 increases this association, we next began evaluating the effects of a kinase on regulating the spinophilin/NF-M association. PKA has been shown in previous studies to phosphorylate spinophilin (Hsieh-Wilson *et al.*

2003). In order to examine the consequences of increased phosphorylation on the interaction between NF-M and spinophilin, endogenous PKA in HEK293 cells was activated through the use of IBMX, a phosphodiesterase inhibitor (Corbin and Francis 2001) and forskolin, an adenylyl cyclase activator (Seamon and Daly 1980). Data previously obtained suggest that there is a decrease in the interaction between spinophilin and NF-M in a mouse model of PD (Fig. 11). In accordance with these findings, a reduction in the level of NF-M in spinophilin IPs was found when endogenous PKA was activated over a short time course (30 minutes). The same was found when levels of spinophilin in NF-M IPs were examined. Unexpectedly, there was no change in the level of spinophilin phosphorylation after PKA activation at the known PKA site, Ser100 as analyzed by mass spectrometry. However, there was an increase in the level of NF-M phosphorylation under these conditions.

Conversely, long-term activation of PKA (16-20 hours) increases the NF-M/spinophilin interaction. These unexpected data suggest that PKA may be playing multiple roles in regulating the interaction between NF-M and spinophilin. It is possible that the different time courses of activation leads to NF-M phosphorylation at different sites or that long-term pharmacological treatment leads to compensatory changes. A more recent study has used computer models to predict PKA phosphorylation sites on spinophilin including serines 87, 94, 99, 100, 122, and 126 (Xue *et al.* 2005). Interestingly, similar to the short-term activation study outlined above, there was no increase in spinophilin phosphorylation upon long-term endogenous PKA activation, at least at the known PKA site, Ser100. It is possible that additional sites on spinophilin tryptic peptides that were not detected in our analysis are being hyper-phosphorylated.

Future studies will need to further analyze spinophilin phosphorylation upon PKA-dependent activation under both long-term and short-term activation conditions.

Interestingly, MS/MS data indicate various changes in the phosphorylation state of NF-M at specific serine residues. Therefore, changes in NF-M phosphorylation may be modulating the association between spinophilin and NF-M. Interestingly, there appears to be fairly striking differences in an initial proteomics screen evaluating the phosphorylation status of NF-M under short-term compared to long-term activation. Specifically, phosphorylation of multiple residues on NF-M increased or remained at control levels in samples where a short-term PKA activation took place

We observed increased phosphorylation of spinophilin at Ser100 in an animal model of PD. However, it is unclear the mechanisms that are linked to this altered phosphorylation. One putative, spinophilin-dependent mechanism may involve modulation of spinophilin with various G-protein-coupled receptors (GPCRs). Spinophilin has been shown to associate with the dopamine D_2 receptor and the α2A adrenergic receptor (Smith *et al.* 1999; Wang and Limbird 2002). Furthermore, it has been shown that spinophilin knockout can enhance coupling of GPCRs to their G-proteins and can modulate the actions of arrestins to modulate GPCR levels (Wang *et al*., 2004; Lu *et al.* 2010). The association of spinophilin with the dopamine D_2 receptor, may position this molecule in close proximity to the D_2 receptor and to downstream adenylyl cyclase and PKA. Given that PD is associated with loss of dopamine and disinhibition of adenylyl cyclase, we hypothesize that this may be one mechanism by which spinophilin is hyper-phosphorylated at the Ser100 site. Future studies will need to specifically test this hypothesis.

4.4 *In Vitro* Phosphorylation via PKA Reduces the Interaction between NF-M and Spinophilin

To determine if spinophilin phosphorylation by PKA directly regulates its association with NF-M, we phosphorylated GST-tagged spinophilin fragments with the catalytic subunit of PKA (PKAc) and incubated phosphorylated and mock treated fragments with cortical tissue homogenates. Cortical lysates was also incubated with GST fragments in the absence of PKA. We precipitated the GST proteins, separated SpAPs via SDS-PAGE, and evaluated total SpAPs in the phosphorylated and mock conditions. Interestingly, there was an overall decrease in the relative amount of SpAPs associated with the phosphorylated N-terminal GST-spinophilin fragment. MS/MS data confirm this observation and suggest that phosphorylation of spinophilin via PKA is responsible for attenuating the interaction between spinophilin and a swath of structural proteins (Table 2). While we have begun to validate these changes with NF-M, future studies will need to evaluate some of the other proteins (e.g. myosins) that also appear to be regulated by spinophilin phosphorylation.

4.5 Mutation of Specific Amino Acid Residues Reduces the Interaction between NF-M and Spinophilin

As was previously discussed, PKA phosphorylates spinophilin at Ser100 (Hsieh-Wilson *et al.* 2003). Additionally, Cdk5 phosphorylates spinophilin at Ser17 (Futter *et al.* 2005). In order to examine the specific effects of phosphorylation at these sites, GST-tagged spinophilin mutants were generated containing amino acid residues 1-154. Fragments containing Ser17Ala, Ser17Asp, Ser100Ala, or Ser100Asp mutations as well

as Ser17/100Ala and Ser17/100Asp were produced. As was expected based on previous data, fragments where both residues were mutated to aspartic acid (phosphorylation-mimicking; Bornancin and Parker 1997) decreased the interaction between spinophilin and NF-M. Taken together, these data suggest that phosphorylation of spinophilin at both Ser17 and Ser100 via Cdk5 and PKA, respectively, will reduce the interaction between NF-M and spinophilin.

However, single mutants, regardless of which mutation or site, yielded variable results. In addition, double mutants containing alanine (an amino acid that cannot be phosphorylated; Bornancin and Parker 1997) at both Ser17 and Ser100 would be expected to increase the level of NF-M in spinophilin pull-downs, as we have seen that absence of phosphorylation enhances the interaction between spinophilin and NF-M (as discussed in section 3.5.1). However, this double mutation (Ser17/100Ala) also produced variable results and actually trended towards a decrease in association. A likely explanation is that because of this fragment's small size, the changing of two amino acids may lead to protein misfolding and decrease the association with NF-M. Continuation of these types of experiments will require the implementation of more robust methods. Further studies wherein full-length spinophilin has been mutated may also be useful in order to further validate these findings.

Also of importance is the increase in spinophilin phosphorylation at Ser17 and Ser100 in 6-OHDA lesioned mice (Fig. 18). However, the experiments described in this section only take into account human spinophilin fragments while simultaneously utilizing cortical tissue obtained from mice. Therefore, it was necessary to verify sequence similarity among species. As Uniprot sequence alignment revealed, both Ser17

and Ser100 are conserved among mouse, rat, and human (Fig. 20), implying that the aforementioned phosphorylation events in animal models might also occur in human PD patients.

4.6 Overexpression of PKA Enhances the Interaction between NF-M and Spinophilin

We showed that short-term and long-term activation of PKA led to decreased and increased association between spinophilin and NF-M, respectively. While these differences may be due to differences in phosphorylation of NF-M (see above) an alternative hypothesis is that long-term activation leads to greater levels of free PKAc. To test the effect of enhanced free PKAc, we overexpressed spinophilin and/or NF-M in the absence or presence of a myc-tagged PKAc. Interestingly, overexpression of PKAc caused a very robust increase in the association of NF-M and spinophilin. As discussed above, this increased association might be due to substantively greater or different phosphorylation in the presence of a high abundance of PKAc. In spinophilin IPs where PKA was also overexpressed, several phosphorylation sites were detected via MS/MS. Specifically, we found that there was greater phosphorylation of spinophilin at Ser100, Ser116, Ser126, and Ser203. Interestingly, two PKA phosphorylation sites (Ser100 and 126; Hsieh-Wilson *et al.* 2003) were detected in the absence of overexpressed PKA, suggesting some endogenous low-level of kinase activity; however, phosphorylation of both of these sites increased upon PKA overexpression. Of the additional sites that become phosphorylated when PKA is overexpressed, many of them are actually predicted Cdk5 phosphorylation sites (Xue *et al.* 2005). These data diverge from data found when activating PKA, where no change in spinophilin phosphorylation was seen. In addition to

spinophilin, NF-M phosphorylation at Ser346 and Ser736 was higher upon overexpression of PKA. Both of these sites were increased following short-term activation of PKA in HEK293 cells, albeit to much lower extents. However while the Ser346 site is slightly increased following long-term activation, the Ser736 site was actually decreased.

While phosphorylation of spinophilin at sites such as Ser116 and Ser203 in HEK293 cells in the presence of high levels of PKA may be the cause of the increased association between spinophilin and NF-M in these conditions, another possible mechanism would be PKAc bridging the interaction between spinophilin and NF-M. Interestingly, PKAc was observed in both NF-M and spinophilin immunoprecipitates. Therefore, overexpression of PKA may result in enhanced bridging between the two proteins. Moreover, long-term kinase activity may lead to either greater PKAc levels and/or different NF-M phosphorylation states compared to the short-term activation.

To test if bridging *per se* can modulate the association between spinophilin and NF-M, we incubated purified spinophilin with purified PKAc in the absence or presence of ATP. Interestingly, there was an overall increase in the association of NF-M and spinophilin when PKAc is present but inactive (due to absence of ATP and EDTA) versus samples where PKAc is absent. Qualitative data indicate a very low association of NF-M and spinophilin in the absence of PKAc when samples were analyzed via Western blot. In samples where PKAc is active, this association remains similar. Taken together, these data suggest that the catalytic subunit of PKA, is bridging the interaction between NF-M and spinophilin when inactive. This is somewhat surprising as the amount of PKAc used in these *in vitro* phosphorylation experiments is extremely low. Further

studies will need to examine the effects of PKA in this context. Furthermore, there was a trend for an increase in the association of NF-M with spinophilin when NF-M was pre-incubated with active or non-active PKAc. Taken together, our data suggest that increases in the spinophilin/NF-M association may be due to a bridging effect of free PKAc rather than PKAc activity. However, PKAc activity may attenuate the ability of the catalytic subunit to bind to spinophilin. To our knowledge, these exciting data are the first to show a bridging role for inactive PKA. It is unclear if PKAc is sufficient to bridge the interaction between spinophilin and NF-M or if additional protein(s) are involved.

4.7 Functional Implications in Spinophilin/NF-M association

Interestingly, when spinophilin was co-expressed with NF-M, there was an increase in the phosphorylation of NF-M at Ser30. While PKA activation *per se* did not modulate phosphorylation at this site, the spinophilin-dependent increase in phosphorylation at this site was attenuated by both short-term and long-term activation of PKA. It is unclear why spinophilin increases NF-M phosphorylation at this site in the absence of PKA. Interestingly, in addition to PP1, spinophilin has been shown to associate with CaMKII (Baucum et al., 2012). It is possible that spinophilin is targeting CaMKII or another kinase to NF-M to regulate its phosphorylation. Moreover, upon PKA activation, the association between spinophilin and NF-M is attenuated as is the increased NF-M phosphorylation at this site. Interestingly, multiple other sites on NF-M were increased by PKA phosphorylation. These include peptides containing Ser346, 615, 620, 633, 641, 646, 654, 657, 659, 680, 685, 736, and 837. Given the repeat structure of NF-M, phosphorylation is detected on two identical peptides and therefore may be occurring

at multiple sites on NF-M. While PKA increased phosphorylation at these peptides, spinophilin normalized the phosphorylation at some of these sites. This suggests a functional role of spinophilin in modulating the phosphorylation of NF-M by spinophilin.

In contrast to the short-term phosphorylation, long-term PKA activation had variable effects on different residues, including both increasing and decreasing phosphorylation. Interestingly, phosphorylation of the tryptic peptide containing Ser620 and Ser685 was increased by overnight expression of PKA and this phosphorylation was attenuated by co-expression of spinophilin. One possible explanation for these data is that spinophilin is targeting PP1 to NF-M to modulate specific residues. While these data are preliminary, they are very exciting as they suggest a functional role for spinophilin in modulating NF-M phosphorylation.

4.8 Summary

Data presented here suggest that the interaction between spinophilin and NF-M is regulated by phosphorylation as well as PP1 and PKA expression. Specifically, dephosphorylation via PP1, phosphorylation via PKA (and potentially Cdk5), and expression of PKA modulate this interaction. First, we verified that spinophilin and NF-M interact in brain tissue lysates as well as when both proteins are overexpressed in heterologous cell lines. We also established that PP1 increases the interaction between spinophilin and NF-M. PP1 has been shown to coimmunoprecipitate with both spinophilin and NF-M, suggesting that all three may exist in the same complex.

We have also found that phosphorylation via PKA attenuates the interaction between spinophilin and NF-M under certain conditions. Specifically, PKA-dependent

phosphorylation of spinophilin fragments reduces binding of these fragments to NF-M when compared to mock-transfected controls. Furthermore, a short-term activation of endogenous PKA in HEK293 cells decreases the level of NF-M in spinophilin IPs. Point mutations that mimic phosphorylation of spinophilin at one PKA site and one Cdk5 site also indicate a decrease in the association of NF-M and spinophilin. However, when long-term activation of PKA is conducted and when PKAc is overexpressed in this same cell system, there is a significant increase in the association between NF-M and spinophilin. Taken together, these data suggest the existence of two different mechanisms by which the NF-M/spinophilin interaction can be regulated.

The functional implications in modulating the spinophilin/NF-M interaction are unclear. It is possible that low levels of PKA activity or free PKAc may attenuate the spinophilin/NF-M association in order to maintain the phosphorylation of NF-M at higher levels. Conversely, very high levels of PKAc may be triggering a greater association of spinophilin with NF-M in order to enhance the targeting of PP1 to NF-M to balance out very high PKA activity.

4.9 Conclusion and Future Directions

PD is characterized by the loss of nigrostriatal dopaminergic neurons. Dopamine depletion in the striatum may disinhibit PKA activation in dopamine D_2 receptor-containing neurons, enhancing PKA activity in this class of MSNs. At the molecular level, there is a rearrangement of the various proteins that reside in the dendritic spines of postsynaptic cells. As suggested by an animal model of PD, two such proteins whose interactions change are spinophilin and NF-M. It is possible that the proper localization

of NF-M by spinophilin is necessary for the proper formation/structure and function of dendritic spines. Attenuation of the association of NF-M and spinophilin may lead to perturbations in spine structure and function.

Our data suggest that PKAc bridges the association between spinophilin and NF-M. To further test this, we plan to purify a 'kinase dead' mutant, wherein a specific amino acid residue has been mutated in order to ablate catalytic activity of the kinase. This will aid in further evaluating the bridging function of PKAc and that this bridging occurs independent of catalytic activity.

Interestingly, mutation of Ser17 and Ser100 to aspartate leads to attenuation of the spinophilin/NF-M association. Given that Ser17 is a CDK5 site, future studies will need to evaluate the role of CDK5-dependent phosphorylation on regulating the spinophilin/NF-M interaction. This could be done by phosphorylating purified spinophilin constructs or by expressing low levels of the Cdk5 activator p25 or p35 (Tang *et al.* 1995) in HEK293 cells.

Additionally, further studies utilizing animal models of PD could be useful in assessing increases and/or decreases in either kinase or phosphatase levels and/or activity. These experiments could also examine differences in spinophilin's interaction with additional IF proteins (i.e. NF-H, etc.) that can affect dendritic spine structure. Additional animal studies might include producing mutants where expression of either spinophilin or NF-M has been knocked out. Whereas NFs have been suggested to affect formation of spines (Lee *et al.* 1987; Yuan *et al.* 2012), they have not yet been studied in this context. We would expect that knockout of single NF protein expression would severely disrupt the formation of spines as well as axons, and therefore, synaptic connectivity.

Immunohistochemical imaging studies using confocal microscopy with tissue extracted from both wild type and mutant animals could help elucidate further questions pertaining to the colocalization of the various proteins discussed herein. These studies could also be conducted in HEK293 cells where spinophilin, NF-M and PP1 or PKA are overexpressed.

We have specifically explored the differences in the interaction between NF-M and spinophilin due to changes made to spinophilin (outside of *in vitro* phosphorylation of full-length NF-M). Future studies might consider some complimentary experiments. For example, identifying the NF-M motif (head, rod, or tail) that specifically interacts with spinophilin will be useful in evaluating the differences in this interaction. Once this has been established, it will be easier to manipulate NF-M and to determine which, if any, alterations to this protein will affect its association with spinophilin.

Overall, the data presented herein reveal important changes in the interaction between two important neuronal proteins. Furthermore, it seems that phosphorylation via PKA as well as its potential bridging effects, have a significant effect on spinophilin's ability to associate with NF-M. The detriment or benefit of these changes has not yet been explored and will require additional studies. It is possible that a decrease in the interaction between NF-M and spinophilin is one of the underlying causes of some of the morphological and behavioral changes observed in PD.

WORKS CITED

WORKS CITED

Albin, R. L., Young, A. B., and Penney, J.B. (1989). The functional anatomy of basal ganglia disorders. *Trends Neurosci.,* **12(10):** 366-75.

Al-Chalabi, A. and Miller, C. C. J. (2003) Neurofilaments and neurological disease. *BioEssays*, **25(4):** 346-355

Allen, P., Ouimet, C. and Greengard, P. (1997). Spinophilin, a novel protein phosphatase 1 binding protein localized to dendritic spines. *Proc. Natl. Acad. Sci.* **94(18):** 9956-9961.

Baucum, A. J., Jalan-Sakrikar, N., Jiao, Y., Gustin, R. M., Carmody, L. C., Tabb, D. L., Ham, A. L., and Colbran, R. J. (2010). Identification and validation of novel spinophilin-associated proteins in rodent striatum using and enhanced *ex vivo* shotgun proteomics approach. *Mol. Cell. Prot.,* **9(6):** 1243-1259.

Baucum, A. J., Strack, S., and Colbran, R. J. (2012) Age-dependent targeting of protein phosphatase 1 to Ca^{2+}/calmodulin-dependent protein kinase II by spinophilin in mouse striatum. PLoS ONE **7(2):** e31554. doi:10.1371/journal.pone.0031554

Baucum, A. J., Shonesy, B. C., Rose, K. L., and Colbran, R. J. (2015). Quantitative proteomics analysis of CaMKII phosphorylation and the CaMKII interactome in the mouse forebrain. *ACS Chem. Neurosci.*

Baumann, K., Mandelkow, E. M., Piwnica-Worms, H., and Mandelkow, E. (1993). Abnormal Alzheimer-like phosphorylation of tau-protein by cyclin-dependent kinases cdk2 and cdk5. *FEBS Lett.,* **336(3):** 417-424.

Bear, M. F. (1999). Homosynaptic long-term depression: A mechanism for memory? *Proc. Nat. Acad. Sci.*, **96(17):** 9457-9458.

Berridge, M. J. (2006). Calcium microdomains: organization and function. *Cell Calcium*, **40(5):** 405-412.

Betts, J. C., Blackstock, W. P., Ward, M. A., and Anderton, B. H. (1997). Identification of phosphorylation sites on neurofilament proteins by nanoelectrospray mass spectrometry. *J. Biol. Chem.*, **272(20):** 12922-12927.

Bibb, J. A., Nishi, A., O'Callaghan, J. P., Ule, J., Lan, M., Snyder, G. L., Horiuchi, A., Saito, T., Hisanaga, S-. I., Czernik, A. J., Nairn, A. C., and Greengard, P. (2001). Phosphorylation of protein phosphatase inhibitor-1 by Cdk5. *J. Biol. Chem.*, **276(17):** 14490-14497.

Bibb, J. A., Snyder, G. L., Nishi, A., Yan, Z., Meijer, L., Fienberg, A. A., Tsai, L-. H., Know, Y. T., Girault, J-. A. Czernik, A. J., Huganir, R. L., Hemmings Jr., H. C., Nairn, A. C., and Greengard, P. (1999). Phosphorylation of DARPP-32 by Cdk5 modulates dopamine signalling in neurons. *Nature*, **402(6762):** 669-671.

Björklund, A., and Lindvall, O. (1975). Dopamine in dendrites of substantia nigra neurons: suggestions for a role in dendritic terminals. *Brain Res.*, **83(3):** 531-537.

Bliss, T. V., and Collingridge, G. L. (1993). A synaptic model of memory: long-term potentiation in the hippocampus. *Nature*, **361(6407):** 31-39.

Bocquet, A., Berges, R., Frank, R., Robert, P., Peterson, A. C., and Eyer, J. (2009). Neurofilaments bind tubulin and modulate its polymerization. *J. Neurosci.*, **29(35):** 11043-11054.

Bollen, M., Peti, W., Ragusa, M. J., and Beullens, M. (2010). The extended PP1 toolkit: designed to create specificity. *Trends Biochem. Sci.*, **35(8):** 450-458.

Bornancin, F., and Parker, P. J. (1997). Phosphorylation of protein kinase C-α on serine 657 controls the accumulation of active enzyme and contributes to its phosphatase-resistant state. *J. Biol. Chem.*, **272(6):** 3544-3549.

Brown, A. M., Baucum, A. J., Bass, M. A., and Colbran, R. J. (2008). Association of protein phosphatase $1\gamma_1$ with spinophilin suppresses phosphatase activity in Parkinson disease model. *J. Biol. Chem.*, **283(21):** 14286-14294.

Brown, A. M., Deutch, A. Y., and Colbran, R. J. (2005). Dopamine depletion alters phosphorylation of striatal proteins in a model of Parkinsonism. *Euro. J. Neurosci.*, **22(1):** 247-256.

Cajal, R.S. (1888). Estructura de los centros nerviosos de las aves. *Rev. Trim. Histol. Norm. Pat.* **1:** 1-10.

Calabresi, P., Maj R., Pisani A., Mercuri N. B., Bernardi, G. (1992). Long-term synaptic depression in the striatum: physiological and pharmacological characterization. *J. Neurosci*., **12(11):** 4224-4233.

Carden, M. J., Schlaepfer, W. W., and Lee, V. M.-Y. (1984). The structure, biochemical properties, and immunogenicity of neurofilament peripheral regions are determined by phosphorylation state. *J. Biol. Chem.*, **260(17):** 9805-9817.

Carmody, L. C., Baucum II, A. J., Bass, M. A., and Colbran, R. J. (2008). Selective targeting of the γ1 isoform of protein phosphatase 1 to F-actin in intact cells requires multiple domains in spinophilin and neurabin. *Faseb J.*, **22(6):** 1660-1671.

Cenci, M. A., Lee, C. S., and Björklund, A. (1998). L-DOPA-induced dyskinesia in the rat is associated with striatal overexpression of prodynorphin-and glutamic acid decarboxylase mRNA. *Euro. J. Neurosci.*, **10(8):** 2694-2706.

Ceulemans, H., and Bollen, M. (2006). A tighter RVxF motif makes a finer Sift. *Chem. Biol.*, **13(1):** 6-8.

Ching, G.Y. and Liem, R. K. H. (2006). Neuronal intermediate filaments and neurodegenerative diseases. *Intermediate Filaments*. 35-51.

Cingolani, L. A., and Goda, Y. (2008) Actin in action: the interplay between the actin cytoskeleton and synaptic efficacy. *Nat. Rev. Neurosci.*, **9(5):** 344-356.

Cleverley, K. E., Betts, J. C., Blackstock, W. P., Gallo, J. M., and Anderton, B. H. (1998). Identification of novel *in vitro* PKA phosphorylation sites on the low and middle molecular mass neurofilament subunits by mass spectrometry. *Biochem.*, **37(11):** 3917-3930.

Cohen, P. (1992). Signal integration at the level of protein kinases, protein phosphatases and their substrates. *Trends Biochem. Sci.*, **17(10):** 408-413.

Cohen, P. T. W. (2002). Protein phosphatase 1 – targeted in many directions. *J. Cell Sci.*, **115:** 241-256.

Collard J.F., Cote F., and Julien J.P. (1995). Defective axonal transport in a transgenic mouse model of amyotrophic lateral sclerosis. *Nature*, **375(6526):** 61–64.

Corbin, J. D., and Francis, S. H. (2001). Pharmacology of phosphodiesterase-5 inhibitors. *Int. J. Clin. Pract.*, **56(6):** 453-459.

Dauer, W. and Przedborski, S. (2003). Parkinson's disease: mechanisms and models. *Neuron*, **39(6):** 889-909.

Day, M., Wang, Z., Ding, J., An, X., Ingham, C. A., Shering, A. F., Wokosin, D., Ilijic, E., Sun, Z., Sampson, A. R., Mugnaini, E., Deutch, A. Y., Sesack, S. R., Arbuthnott, G. W., and Surmeier, D. J. (2006). Selective elimination of glutamatergic synapses on striatopallidal neurons in Parkinson disease models. *Nature Neurosci.*, **9(2):** 251-259.

Deep-Brain Stimulation for Parkinson's Disease Study Group. (2001). Deep-brain stimulation of the subthalamic nucleus or the pars interna of the globus pallidus in Parkinson's disease. *N. Engl. J. Med.*, **345(13):** 956.

Dhavan, R., and Tsai, L. H. (2001). A decade of CDK5. *Nat. Rev. Mol. Cell Biol.*, **2(10):** 749-759.

Egloff, M. P., Johnson, D. F., Moorhead, G., Cohen, P. T., Cohen, P., and Barford, D. (1997). Structural basis for the recognition of regulatory subunits by the catalytic subunit of protein phosphatase 1. *The EMBO Journal*, **16(8):** 1876-1887.

Evans, J. C., Robinson, C. M., Shi, M., and Webb, D. J. (2015). The Guanine Nucleotide Exchange Factor (GEF) Asef2 Promotes Dendritic Spine Formation via Rac Activation and Spinophilin-Dependent Targeting. *J. Biol. Chem.*, Jbc-M114.

Feng, J., Yan, Z., Ferreira, A., Tomizawa, K., Liauw, J. A., Zhuo, M., Allen, P. B., Ouimet, C. C., and Greengard, P. (2000). Spinophilin regulates the formation and function of dendritic spines. *Proc. Natl. Acad. Sci.*, **97(16):** 9287-9292.

Fienberg, A. A., Hiroi, N., Mermelstein, P. G., Song, W. J., Snyder, G. L., Nishi, A., Cheramy, A., O'Callaghan, J. P., Miller, D. B., Cole, D. G., Corbett, R., Haile, C. N., Cooper, D. C., Onn, S. P., Grace, A. A., Ouimet, C. C., White, F. J., Hyman, S. E., Surmeier, D. J., Girault, J. –A., Nestler, E. J., and Greengard, P. (1998). DARPP-32: regulator of the efficacy of dopaminergic neurotransmission. *Science*, **281(5378):** 838-842.

Frank, M. J., Seeberger, L. C., and O'Reilly, R. C. (2004). By carrot or by stick: cognitive reinforcement learning in parkinsonism. *Science*, **306(5703):** 1940–1943.

Futter, M., Uematsu, K., Bullock, S. A., Kim, Y., Hemmings, H. C., Nishi, A., Greengard, P., and Nairn, A. C. (2005). Phosphorylation of spinophilin by ERK and cyclin-dependent PK 5 (Cdk5). *Proc. Nat. Acad. Sci.*, **102(9):** 3489-3494.

Garcia, M. L., Rao, M. V., Fujimoto, J., Garcia, V. B., Shah, S. B., Crum, J., Gotow, T., Uchiyama, Y., Ellisman, M., Calcutt, N. A., and Cleveland, D. W. (2009). Phosphorylation of highly conserved neurofilament medium KSP repeats is not requirred for myelin-dependent radial axonal growth. *J. Neurosci.*, **29(5):** 1277-1284.

Gerfen, C. R. and Surmeier, D. J. (2011). Modulation of striatal projection systems by dopamine. *Annu. Rev. Neurosci.* **34:** 441-66.

German, D. C., Manaye, K., Smith, W. K., Woodward, D. J., and Saper, C. B. (1989). Midbrain dopaminergic cell loss in Parkinson's disease: computer visualization. *Annals of Neurology*, **26(4):** 507-514.

Gibb, W. R. and Lees, A. J. (1988). The relevance of the Lewy body to the pathogenesis of idiopathic Parkinson's disease. *J. Neurol., Neurosurg. Psychiatry*, **51(6):** 745-752.

Gou, J. P., Gotow, T., Janmey, P. A., and Leterrier, J. F. (1998). Regulation of neurofilament interactionsin vitro by natural and synthetic polypeptides sharing Lys-Ser-Pro sequences with the heavy neurofilament subunit NF-H: Neurofilament crossbridging by antiparallel sidearm overlapping. *Med. Biol. Eng. Comput.*, **36(3):** 371-387.

Gray, E. G. (1959). Axo-somatic and axo-dendritic synapses of the cerebral cortex: an electron microscope study. *J. Anat.*, **93(Pt 4):** 420.

Grossman, S. D., Futter, M., Snyder, G. L., Allen, P. B., Nairn, A. C., Greengard, P. and Hsieh-Wilson, L.C. (2004). Spinophilin is phosphorylated by Ca^{2+}/calmodulin-dependent protein kinase II resulting in regulation of its binding to F-actin. *J. Neurochem.,* **90(2):** 317-324.

Guan, K. L. and Dixon, J. E. (1991). Eukaryotic proteins expressed in *Escherichia coli*: an improved thrombin cleavage and purification procedure of fusion proteins with glutathione S-transferase. *Analytical Biochem.,* **192(2):** 262-267.

Häusser, M., Spruston, N., and Stuart, G. J. (2000). Diversity and dynamics of dendritic signaling. *Science*, **290(5492):** 739-744.

Hering, H. and Sheng, M. (2001). Dendritic spine: structure, dynamics and regulation. *Nat. Rev. Neurosci.,* **2(12):** 880-888.

Hervé, D., Le Moine, C., Corvol, J. C., Belluscio, L., Ledent, C., Fienberg, A. A., Jaber, M., Studler, J-. M., and Girault, J. A. (2001). $G\alpha_{olf}$ levels are regulated by receptor usage and control dopamine and adenosine action in the striatum. *J. of Neurosci.*, **21(12):** 4390-4399.

Hoffman, P. N. and Lasek, R. J. (1975). The slow component of axonal transport. Identification of major structural polypeptides of the axon and their generality among mammalian neurons. *J. Cell Bio.* **66(2)**, 351-366.

Holman, J. D., Ma, Z. Q., and Tabb, D. L. (2012). Identifying Proteomic LC-MS/MS Data Sets with Bumbershoot and IDPicker. *Curr. Prot. in Bioinformatics*, 13-17.

Hornykiewicz, O. (1974). The mechanisms of action of L-dopa in Parkinson's disease. *Life Sciences*, **15(7):** 1249-1259.

Hsieh-Wilson, L. C., Benfenati, F., Snyder, G. L., Allen, P. B., Nairn, A. C., and Greengard, P. (2003). Phosphorylation of spinophilin modulates its interaction with actin filaments. *J. Biol. Chem.,* **278(2):** 1186-1194.

Ingham, C. A., Hood, S. H., Arbuthnott, G. W. (1989). Spine density on neostriatal neurones changes with 6-hydroxydopamine lesions and with age. *Brain Res.,* **503(2):** 334-338.

Ingham, C. A., Hood, S. H., van Maldegem B., Weenink, A., Arbuthnott, G. W. (1993). Morphological changes in the rat neostriatum after unilateral 6-hydroxydopamine injections into the nigrostriatal pathway. *Exp. Brain Res.,* **93(1):** 17-27.

Janssens, V., Longin, S., and Goris, J. (2008). PP2A holoenzyme assembly: in cauda venenum (the sting is in the tail). *Trends Biochem. Sci.*, **33(3):** 113-121.

Julien, J. P. (1999). Neurofilament functions in health and disease. *Curr. Opin. Neurobiol.,* **9(5):** 554-560.

Kennedy, M. B. (2000). Signal-processing machines at the postsynaptic density. *Science*, **290(5492):** 750-754.

Kim, S., Mischerikow, N., Bandeira, N., Navarro, J. D., Wich, L., Mohammed, S., Heck, A. J. R., and Pevzner, P. A. (2010). The generating function of CID, ETD, and CID/ETD pairs of tandem mass spectra: applications to database search. *Mol. Cell Prot.*, **9(12):** 2840-2852.

Kong J., Tung V.W., Aghajanian J., and Xu Z. (1998). Antagonistic roles of neurofilament subunits NF-H and NF-M against NF-L in shaping dendritic arborization in spinal motor neurons. *J. Cell Biol.* **140(5):**1167–1176.

Krüger, R., Fischer, C., Schulte, T., Strauss, K. M., Müller, T., Woitalla, D., Berg, D., Hungs, M., Gobbele, R., Berger, K., Epplen, J. T., Riess, O., and Schöls, L. (2003). Mutation analysis of the neurofilament M gene in Parkinson's disease. *Neurosci. Lett.*, **351(2):** 125-129.

Kumar, R., Lozano, A. M., Kim, Y. J., Hutchison, W. D., Sime, E., Halket, E., and Lang, A. E. (1998). Double-blind evaluation of subthalamic nucleus deep brain stimulation in advanced Parkinson's disease. *Neurology*, **51(3):** 850-855.

Lee, V. M., Carden, M. J., Schlaepfer, W. W. and Trojanowski, J. Q. (1987). Monoclonal antibodies distinguish several differentially phosphorylated states of the two largest rat neurofilament subunits (NF-H and NFM) and demonstrate their existence in the normal nervous system of adult rats. *J. Neurosci*., **7(11):** 3474-3488.

Lesage, S., Durr, A., Tazir, M., Lohmann, E., Leutenegger, A. L., Janin, S., Pollak, P., and Brice, A. (2006). *LRRK2* G2019S as a cause of Parkinson's disease in North African Arabs. *N. Engl. J. Med.*, **354(4):** 422-423.

Lewy, F. H. (1912). Paralysis agitans. I Pathologische anatomie. *Handbuch der Neurologie*, ed. Lewandowsky, M. 920-933.

Liu, W., Yuen, E. Y., Allen, P. B., Feng, J., Greengard, P., and Yan, Z. (2006). Adrenergic modulation of NMDA receptors in prefrontal cortex is differentially regulated by RGS proteins and spinophilin. *Proc. Nat. Acad. Sci.*, **103(48):** 18338-18343.

Lynch, D. R., and Guttmann, R. P. (2001). Excitotoxicity: perspectives based on *N*-methyl-D-aspartate receptor subtypes. *J. Pharmacol. Exp. Ther*., **300(3):** 717-723.

Lu, R., Chen, Y., Cottingham, C., Peng, N., Jiao, K., Limbird, L. E., Wyss, J. M., and Want, Q. (2010). Enhanced hypotensive, bradycardic, and hypnotic responses to α_2-adrenergic agonists in spinophilin-null mice are accompanied by increased G protein coupling to the α_{2A}-adrenergic receptor. *Mol. Pharmacol.*, **78(2):** 279-286.

Malenka, R. C., and Bear, M. F. (2004). LTP and LTD: an embarrassment of riches. *Neuron*, **44(1):** 5-21.

Manning, G., Whyte, D. B., Martinez, R., Hunter, T., and Sudarsanam, S. (2002). The protein kinase complement of the human genome. *Science*, **298(5600):** 1912-1934.

Massey, P. V., and Bashir, Z. I. (2007). Long-term depression: multiple forms and implications for brain function. *Trends Neurosci.*, **30(4):** 176-184.

McNeill, T. H., Brown, S. A., Rafols, J. A. and Shoulson, I. (1988). Atrophy of medium spiny I striatal dendrites in advanced Parkinson's disease. *Brain Res*., **455(1):** 148-152.

Meiselback, H., Sticht, H., and Enz, R. (2006). Structural analysis of the protein phosphatase 1 docking motif: molecular description of binding specificities identifies interacting proteins. *Chem. Biol.*, **13(1):** 49-59.

Meraldi, P., and Nigg, E. A. (2001). Centrosome cohesion is regulated by a balance of kinase and phosphatase activities. *J. Cell Sci.*, **114(20):** 3749-3757.

Muly, E. C., Allen, P, Mazloom, M., Aranbayeva, Z., Greenfield, A. T., and Greengard, P. (2004). Subcellular distribution of neurabin immunolabeling in primate prefrontal cortex: comparison with spinophilin. *Cerebral Cortex* **14(12):** 1398-1407.

Nakanishi, H., Obaishi, H, Satoh, A., Wada, M., Mandai, K., Satoh, K., Nishioka, H., Matsuura, Y., Mizoguchi, A, and Takai, Y. (1997). Neurabin: A novel neural tissue-specific actin filament-binding protein involved in neurite formation. *J. Cell Biol.*, **139(4):** 951-961.

Nishi, A., Kuroiwa, M., Miller, D. B., O'Callaghan, J. P., Bateup, H. S., Shuto, T., Sotogaku, N., Fukuda, T., Heintz, N., Greengard, P., and Snyder, G. L. (2008). Distinct roles of PDE4 and PDE10A in the regulation of cAMP/PKA signaling in the striatum. *J. Neurosci.*, **28(42):** 10460-10471.

Oh, J. D., Dotta, P. D., and Chase, T. N. (1997). Protein kinase A inhibitor attenuates levodopa-induced motor response alterations in the hemi-parkinsonian rat. *Neurosci. Lett.*, **228(1):** 5-8.

Ohshima, T., Ward, J. M., Huh, C. G., Longenecker, G., Veeranna, Pant, H. C., Brady, R. O., Marin, L. J., and Kulkarni, A. B. (1996). Targeted disruption of the cyclin-dependent kinase 5 gene results in abnormal corticogenesis, neuronal pathology and perinatal death. *Proc. Natl. Acad. Sci.* **93(20):** 11173-11178.

Parkinson, J. (1817). An essay on the shaking palsy. London: Whittingham & Rowland.

Pearce, R. K. B., Jackson, M., Smith, L., Jenner, P., and Marsden, C. D. (1995). Chronic L-DOPA administration induces dyskinesias in the 1-methyl-4-phenyl-1, 2, 3, 6-tetrahydropyridine-treated common marmoset (Callithrix jacchus). *Movement Disorders*, **10(6):** 731-740.

Picconi, B., Gardoni, F., Centonze, D., Mauceri, D., Cenci, M. A., Bernardi, G., Calabresi, P., and Di Luca, M. (2004). Abnormal Ca2+-calmodulin-dependent protein kinase II function mediates synaptic and motor deficits in experimental parkinsonism. *J. Neurosci.*, **24(23):** 5283-5291.

Polymeropoulos, M. H., Lavedan, C., Leroy, E., Ide, S. E., Dehejia, A., Dutra, A., Pike, B., Root, H., Rubenstein, J., Boyer, R., Stenroos, E. S., Chandrasekharappa, S., Athanassiadou, A., Papapetropoulos, T., Johnson, W. G., Lazzarini, A. M., Duvoisin, R. C., Di Lorio, G., Golbe, L. I., and Nussbaum, R. L. (1997). Mutation in the α-synuclein gene identified in families with Parkinson's disease. *Science*, **276(5321):** 2045-2047.

Qu, L., Wang, Y., Zhang, H. T., Li, N., Wang, Q., Yang, Q., Gao, G. D., and Wang, X. L. (2014). 6-OHDA induced calcium influx through N-type calcium channel alters membrane properties via PKA pathway in substantia nigra pars compacta dopaminergic neurons. *Neurosci. Lett.*, **575:** 1-6.

Ragusa, M. J., Dancheck, B., Critton, D. A., Nairn, A. C., Page, R., and Peti, W. (2010). Spinophilin directs protein phosphatase 1 specificity by blocking substrate binding sites. *Nat. Struct. Mol. Biol.*, **17(4):** 459-464.

Rao, M. V., Campbell, J., Yuan, A., Kumar, A., Gotow, T., Uchiyama, Y., and Nixon, R. A. (2003). The neurofilament middle molecular mass subunit carboxyl-terminal tail domains is essential for the radial growth and cytoskeletal architecture of axons but not for regulating neurofilament transport rate. *J. Cell Biol.*, **163(5):** 1021-1031.

Raymond, L. A., Blackstone, C. D., and Huganir, R. L. (1993). Phosphorylation of amino acid neurotransmitter receptors in synaptic plasticity. *Trends Neurosci.*, **16(4):** 147-153.

Roche, K. W., Tingley, W. G., and Huganir, R. L. (1994). Glutamate receptor phosphorylation and synaptic plasticity. *Curr. Op. in Neurobio.* **4(3):** 383-388.

Roche, K.W., O'Brien, R. J., Mammen, A. L., Bernhardt, J. and Huganir, R. L. (1996). Characterization of multiple phosphorylation sites on the AMPA receptor GluR1 subunit. *Neuron*, **16(6):** 1179-1188.

Rodriguez-Oroz, M. C., Jahanshahi, M., Krack, P., Litvan, I., Macias, R., Bezard, E., and Obeso, J. A. (2009). Initial clinical manifestations of Parkinson's disease: features and pathophysiological mechanisms. *The Lancet Neurology*, **8(12):** 1128-1139.

Satoh, A., Nakanishi, H., Obaishi, H., Wada, M., Takahashi, K., Satoh, K., Hirao, K., Nishioka, H., Hata, Y., Mizoguchi, A., and Takai, Y. (1998). Neurabin-II/spinophilin an actin filament-binding protein with one pdz domain localized at cadherin-based cell-cell adhesion sites. *J. Biol. Chem.*, **273(6):** 3470-3475.

Schlaepfer, W. W. and Freeman, L. A. (1978). Neurofilament proteins of rat peripheral nerve and spinal cord. *J. Cell Biol.*, **78(3):** 653-662.

Scott, J. D., and Pawson, T. (2009). Cell signaling in space and time: where proteins come together and when they're apart. *Science*, **326(5957):** 1220-1224.

Seamon, K. B., and Daly, J. W. (1980). Forskolin: a unique diterpene activator of cyclic AMP-generating systems. *J. Cyclic Nucleotide Research*, **7(4):** 201-224.

Sharma, M., Sharma, P., and Pant H. C. (1999). CDK-5-mediated neurofilament phosphorylation in SHSY5Y human neuroblastoma cells. *J. Neurochem*. **73(1):** 79-86.

Sheng, M., and Hoogenraad, C. C. (2007). The postsynaptic architecture of excitatory synapses: a more quantitative view. *Annu. Rev. Biochem.*, **76:** 823-847.

Sheng, M., and Kim, M. J. (2002). Postsynaptic signaling and plasticity mechanisms. *Science*, **298(5594):** 776-780.

Shetty, K. T., Link, W. T., and Pant, H. C. (1993). Cdc2-like kinase from rat spinal cord specifically phosphorylates KSPXK motifs in neurofilament proteins: isolation and characterization. *Proc. Nat. Acad. Sci.*, **90(14):** 6844-6848.

Shulman, J. M., De Jager, P. L., and Feany, M. B. (2011). Parkinson's disease: genetics and pathogenesis. *Annu. Rev. Pathol. Mech. Dis.* **6:** 193-222.

Sibley, D. R., and Monsma, F. J. (1992). Molecular biology of dopamine receptors. *Trends Pharmacol. Sci.*, **13:** 61-69.

Sidhu, A. (1998). Coupling of D1 and D5 dopamine receptors to multiple G proteins: implications for understanding the diversity in receptor-G protein coupling. *Mol. Neurobio.*, **16(2):** 125-134.

Sihag, R. K., Jaffe, H., Nixon, R. A., and Rong, X. (1999). Serine-23 is a major protein kinase A phosphorylation site on the amino-terminal head domain of the middle molecular mass subunit of neurofilament proteins. *J. Neurochem.*, **72(2):** 491-499.

Smith, F. D., Oxford, G. S., and Milgram, S. L. (1999). Association of the D2 dopamine receptor third cytoplasmic loop with spinophilin, a protein phosphatase-1-interacting protein. *J. Biol. Chem.*, **274(28):** 19894-19900.

Smith, Y., Bevan, M. D., Shink, E., and Bolam, J. P. (1998). Microcirtuitry of the direct and indirect pathways of the basal ganglia. *Neurosci.* **86(2):** 353-387.

Soderling, T.R. (2000). CaM-kinases: modulators of synaptic plasticity. *Curr. Opin. Neurobio.*, **10(3):** 375-380.

Spillantini, M. G., Schmidt, M. L., Lee, V. M. Y., and Trojanowski, J. Q. (1997). α-Synuclein in Lewy bodies. *Nature*, **388(6645):** 839-840.

Starr, M. S. (1995). Glutamate/dopamine D1/D2 balance in the basal ganglia and its relevance to Parkinson's disease. *Synapse*, **19(4):** 264-293.

Stephens, B., Mueller, A. J., Shering, A. F., Hood, S. H., Taggart, P., Arbuthnott, G. W., Bell, J. E., Kilford, L., Kingsbury, A. E., Daniel, S. E., and Ingham, C. A. (2005). Evidence of a breakdown of corticostriatal connections in Parkinson's disease. *Neurosci.*, **132(3):** 741-754.

Stoof, J. C. and Kebabian, J. W. (1981). Opposing roles for D-1 and D-2 dopamine receptors in efflux of cyclic AMP from the rat neostriatum. *Nature*, **294:** 366-368.

Stoof, J. C., and Kebabian, J. W. (1984). Two dopamine receptors: biochemistry, physiology and pharmacology. *Life Sciences*, **35(23):** 2281-2296.

Strange, P. G. (1993). Dopamine receptors in the basal ganglia: relevance to Parkinson's disease. *Movement Disorders.* **8(3):** 263-270.

Surmeier, D. J., Ding, J., Day, M., Wang, Z., and Shen, W. (2007). D1 and D2 dopamine-receptor modulation of striatal glutamatergic signaling in striatal medium spiny neurons. *Trends Neurosci.*, **30(5):** 228-235.

Svenningsson, P., Nishi, A., Fisone, G., Girault, J. A., Nairn, A. C., and Greengard, P. (2004). DARPP-32: an integrator of neurotransmission. *Annu. Rev. Pharmacol. Toxicol.*, **44:** 269-296.

Tabb, D. L., Fernando, C. G., and Chambers, M. C. (2007). MyriMatch: highly accurate tandem mass spectral peptide identification by multivariate hypergeometric analysis. *J. Prot. Res.*, **6(2):** 654-661.

Tang, D., Yeung, J., Lee, K. Y., Matsushita, M., Matsui, H., Tomizawa, K., Hatase, O., and Wang, J. H. (1995). An isoform of the neuronal cyclin-dependent kinase 5 (Cdk5) activator. *J. Biol. Chem.*, **270(45):** 26897-26903.

Terry-Lorenzo, R. T., Inoue, M., Connor, J. H., Haystead, T. A. J., Armbruster, B. N., Gupta, R. P., Oliver, C. J., and Shenolikar, S. (2000). Neurofilament-L is a protein phosphatase-1-binding protein associated with neuronal plasma membrane and post-synaptic density. *J. Biol. Chem.*, **274(4):** 2439-2446.

Terry-Lorenzo, R. T., Elliot, E., Weiser, D. C., Prickett, T. D., Brautigan, D. L., and Shenolikars, S. (2002) Neurabins recruit protein phosphatase-1 and inhibitor-2 to the actin cytoskeleton. *J. Biol. Chem.*, **277(48):** 46535-46543

Terry-Lorenzo, R. T., Roadcap, D. W., Otsuka, T., Blanpied, T. A., Zamorano, P. L., Garner, C. C., Shenolikar, S., and Ehlers, M. D. (2005). Neurabin/protein phosphatase-1 complex regulates dendritic spine morphogenesis and maturation. *Mol. Biol. Cell*, **16(5):** 2349-2362.

Tingley, W. G., Ehlers, M. D., Kameyama, K., Doherty, C., Ptak, J. B., Riley, C. T., and Huganir, R. L. (1997). Characterization of protein kinase A and protein kinase C phosphorylation of the *N*-methyl-D-aspartate receptor NR1 subunit using phosphorylation site-specific antibodies. *J. Biol. Chem.*, **272(8):** 5157-5166.

Trimpin, S., Mixon, A. E., Stapels, M. D., Kim, M. Y., Spencer, P. S. and Deinzer, M. L. (2004). Identification of endogenous phosphorylation sites of bovine medium and low molecular weight neurofilament proteins by tandem mass spectrometry. *Biochem.*, **43(7):** 2091-2105.

Veeranna, N. D. A., Ahn, N. G., Jaffe, H., Winters, C. A., Grant, P., and Pant, H. C. (1998). Mitogen- activated protein kinases (Erk1,2) phosphorylate lys-ser-pro (KSP) repeats in neurofilament proteins NF-H and NF-M. *J. Neurosci*., **18(1):** 4008—4021.

Villalba, R.M., Lee, H., and Smith, Y. (2009). Dopaminergic denervation and spine loss in the striatum of MPTP-treated monkeys. *Exp. Neurol.*, **215(2):** 220-227.

Wang, Q., and Limbird, L. E. (2002). Regulated interactions of the α2A adrenergic receptor with spinophilin, 14-3-3ζ, and arrestin 3. *J. Biol. Chem.*, **277(52):** 50589-50596.

Wang, Q., Zhao, J., Brady, A. E., Feng, J., Allen, P. B., Lefkowitz, R. J., Greengard, P., and Limbird, L. E. (2004). Spinophilin blocks arrestin actions in vitro and in vivo at G protein-coupled receptors. *Science*, **304(5679):** 1940-1944.

Weisenhorn, D. M. V., Roback, L. J., Kwon, J. H., and Wainer, B. H. (2001). Coupling of cAMP/PKA and MAPK signaling in neuronal cells is dependent on developmental stage. *Exp. Neurology*, **169(1):** 44-55.

Yan, Z., Hsieh-Wilson, L., Feng, J. Tomizawa, K., Allen, P. B., Fienberg, A. A., Nairn, A. C., and Greengard, P. (1999). Protein phosphatase 1 modulation of neostriatal AMPA channels: regulation by DARPP-32 and spinophilin. *Neurosci.*, **2(1):** 13-17.

Yuan, A., Rao, M. V., Sasaki, T., Chen, Y., Kumar, A., Liem, R. K., Eyer, J., Peterson, A. C., Julien, J. P., and Nixon, R. A. (2006). α-internexin is structurally and functionally associated with the neurofilament triplet proteins in the mature CNS. *J. Neurosci.*, **26(39):** 10006-10019.

Yuan, A., Rao, M. V., Veeranna, N. D. A., and Nixon, R. A. (2012). Neurofilaments at a glance. *J. Cell Sci*., **125(14):** 3257-3263.

Yuste R., Majewska A., and Holthoff, K. (2000). From form to function: calcium compartmentalization in dendritic spines. *Nat. Neurosci*., **3:** 653-659.

Xu, H., and Freitas, M. A. (2009). MassMatrix: a database search program for rapid characterization of proteins and peptides from tandem mass spectrometry data. *Proteomics*, **9(6):** 1548-1555.

Xue, Y., Zhou, F., Zhu, M., Ahmed, K., Chen, G., and Yao, X. (2005). GPS: a comprehensive www server for phosphorylation sites prediction. *Nucleic Acids Research*, **33(suppl 2):** W184-W187.

Zito, K., Knott, G., Shepherd, G. M. G., Shenolikar, S., and Svoboda, K. (2004). Induction of spine growth and synapse formation by regulation of the spine actin cytoskeleton. *Neuron*, **44(2):** 321-334.

FIGURES

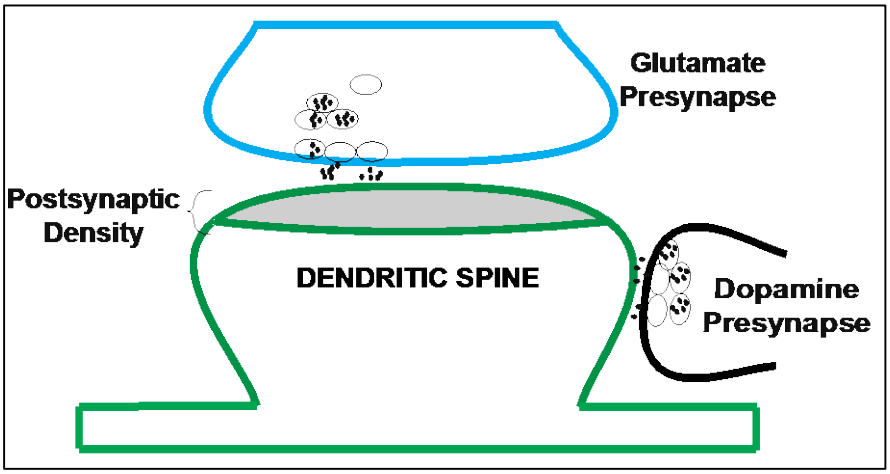

Figure 1: Tripartite system effected in PD. Excitatory glutamatergic neuron projects from the cortex to synapse on the heads of dendritic spines that protrude from striatal MSNs. Dopaminergic neurons project from the substantia nigra to synapse on the neck of dendritic spines. Dopaminergic neurons are lost in PD.

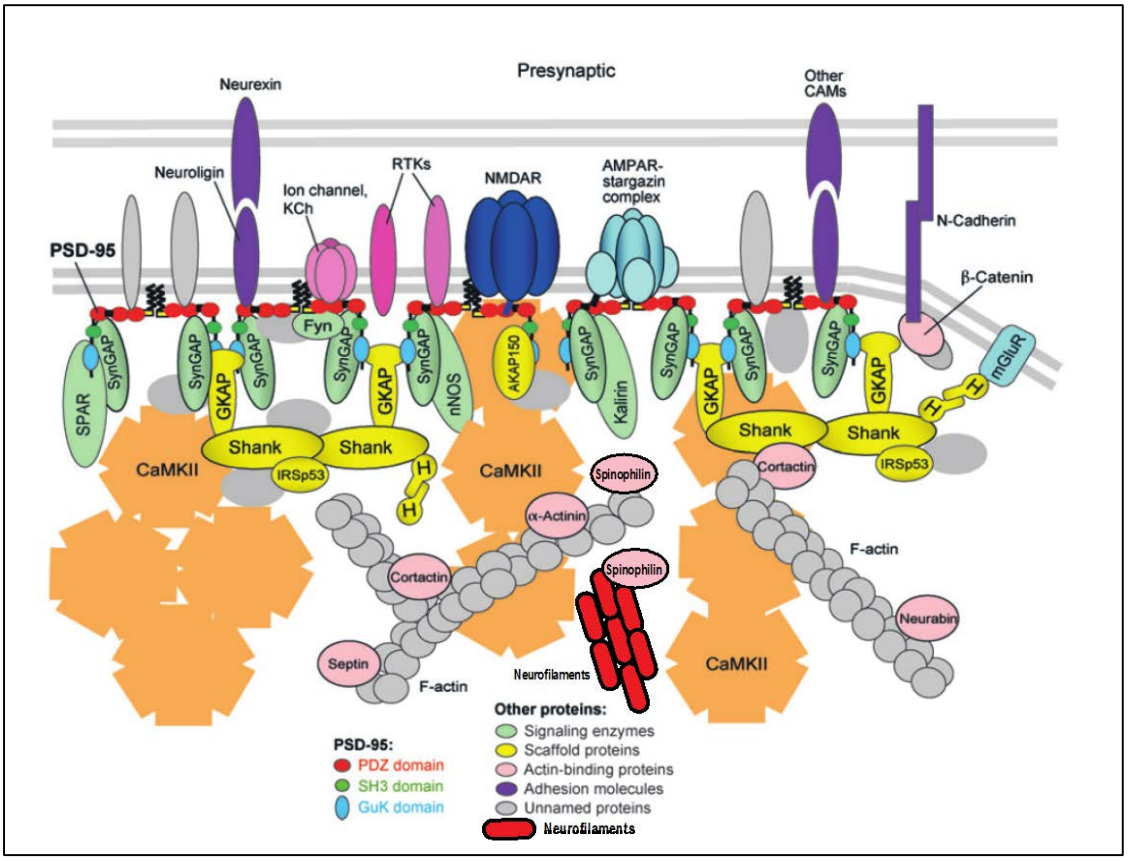

Figure 2: PSD structure. Multiple classes of synaptic proteins interact in a coordinated fashion in order to transduce the signal from the presynaptic glutamatergic neurons. These proteins are critical for normal spine maintenance, signal transduction, and function. Figure adapted from Sheng and Hoogenraad, 2007.

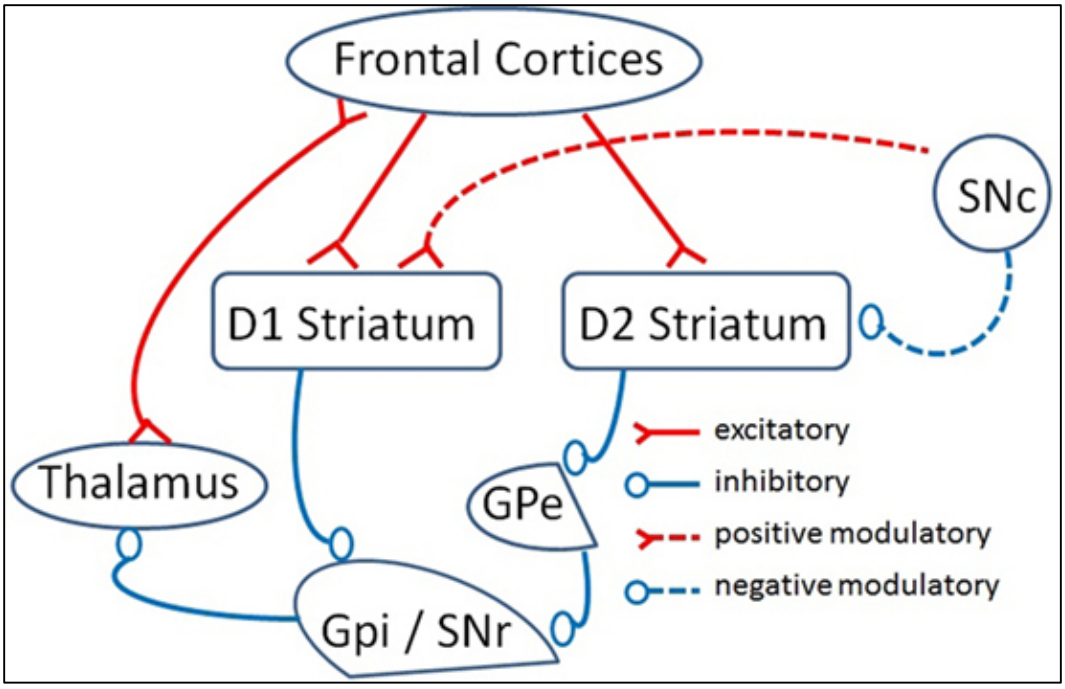

Figure 3: Normal circuitry of the basal ganglia. PD is characterized by the loss of dopaminergic neurons projecting from the substantia nigra (SNc) to the striatum (Frank *et al.* 2004).

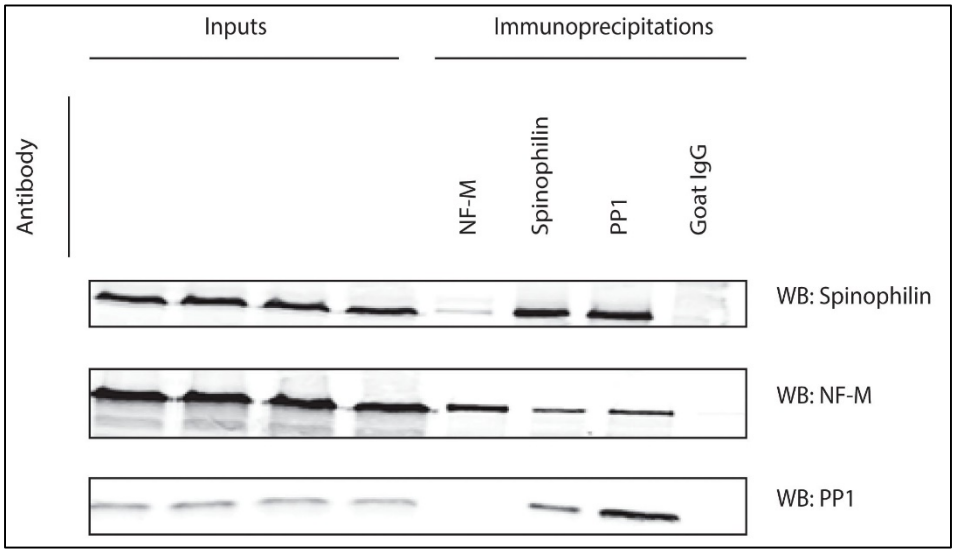

Figure 4: NF-M coimmunoprecipitates with spinophilin and PP1 in cortex. Immunoprecipitations performed using mouse cortical tissue homogenized in a KCl-containing buffer. Immunoprecipitates were blotted using antibodies raised against spinophilin (upper panel), NF-M (middle panel), or PP1 (lower panel).

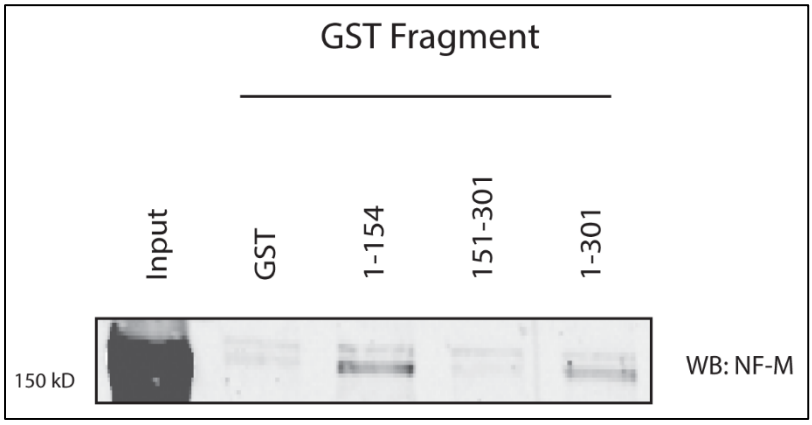

Figure 5: NF-M interacts with spinophilin fragments containing residues 1-154 and 1-301. Cortical lysates were incubated with GST spinophilin fragments. Precipitates were blotted with an NF-M antibody. NF-M associates most strongly with fragments containing spinophilin amino acid residues 1-154 and 1-301.

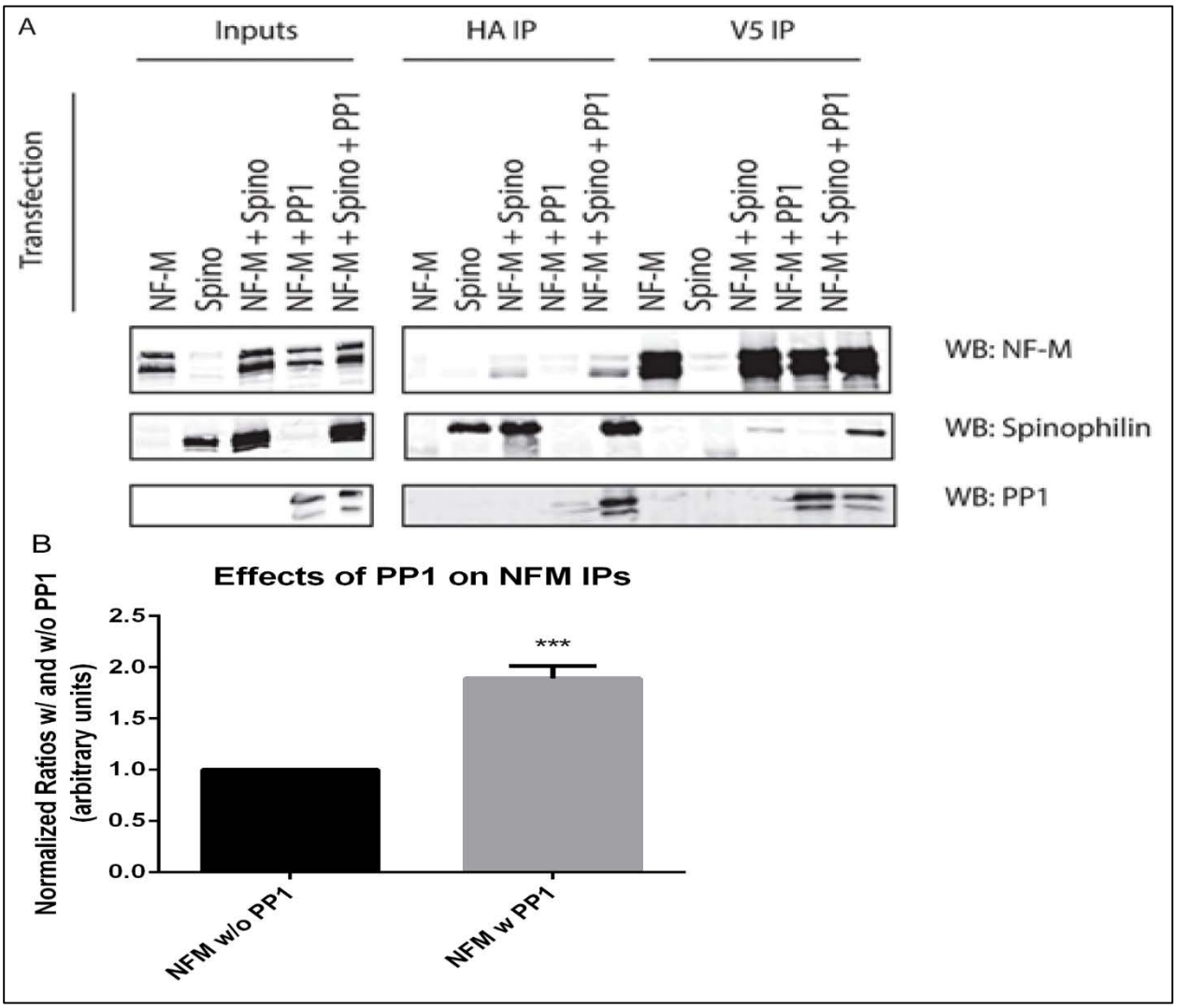

Figure 6: PP1 increases the association of spinophilin and NF-M. A) Western blot of HEK 293 cells transfected with V5-tagged NF-M, HA-tagged spinophilin, and/or PP1γ1. HEK-cell lysates were blotted for antibodies directed against spinophilin, NF-M, and PP1 (left). Immunoprecipitations were performed with rabbit monoclonal antibodies for HA or V5 (right; as noted). Immunoprecipitates were blotted with antibodies for spinophilin, NF-M, and PP1. **B)** Quantified data showing a relative increase in the amount of NF-M in spinophilin IPs when PP1 is co-transfected. $p < 0.001$. $n = 5$.

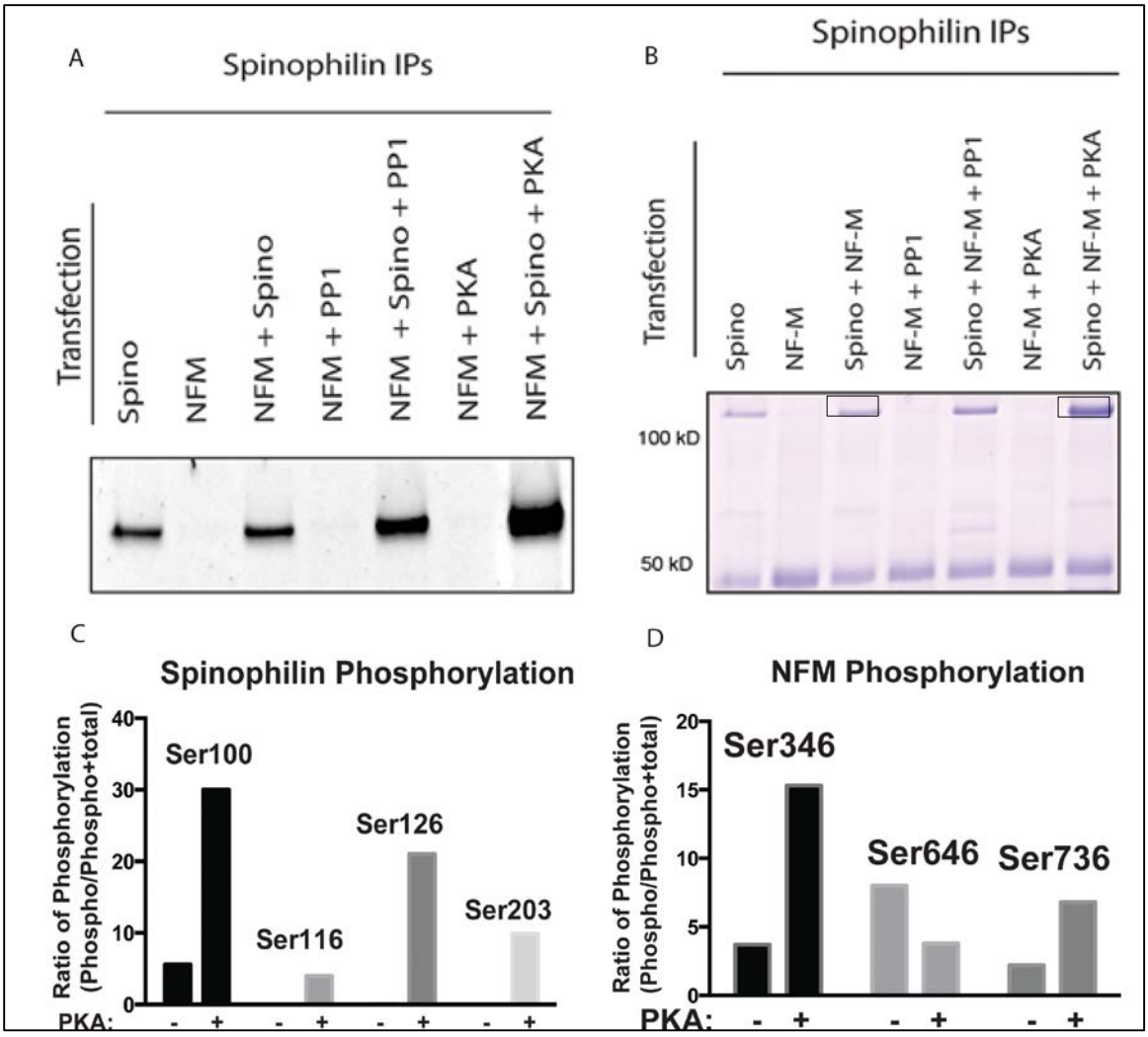

Figure 7: PKA enhances spinophilin phosphorylation. A) HEK 293 cells were transfected as indicated. Immunoprecipitations were performed with antibodies for the HA tag (spinophilin) and samples were separated by SDS-PAGE then stained with Pro-Q Diamond. **B)** Subsequently, gels were post-stained with Imperial stain. **C)** Phosphorylation percentage at specific spinophilin residues in the absence (-) or presence (+) of PKA. **D)** Phosphorylation percentage at specific NF-M residues in the absence (-) or presence (+) of PKA when both proteins are overexpressed. Samples were immunoprecipitated for NF-M.

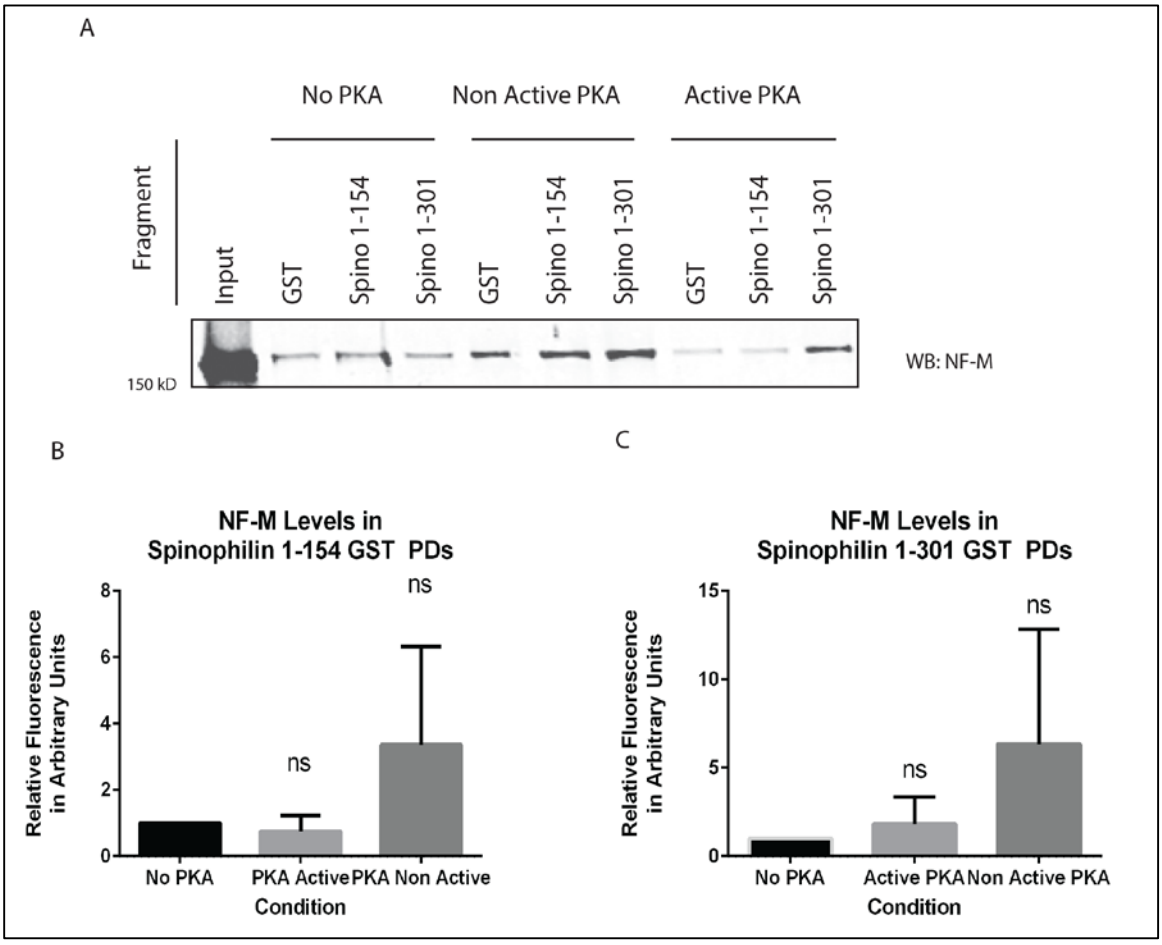

Figure 8: *In vitro* phosphorylation decreases spinophilin fragment association with NF-M. A) Spinophilin fragments were incubated with the catalytic subunit of PKA in the presence (phos.) or absence (mock phos.) of ATP. EDTA was added to each reaction mixture after incubation in order to halt catalytic activity. Spinophilin fragments alone or mock or phosphorylated fragments were incubated with mouse cortical lysates. GST pull-downs were blotted with an NF-M specific antibody. **B)** Quantified data show no significant change in under either condition when lysate was incubated with AA1-154. n = 5; p = 0.1307. **C)** Quantified data show no significant change in under either condition when lysate was incubated with AA1-301. n = 5; p = 0.0999.

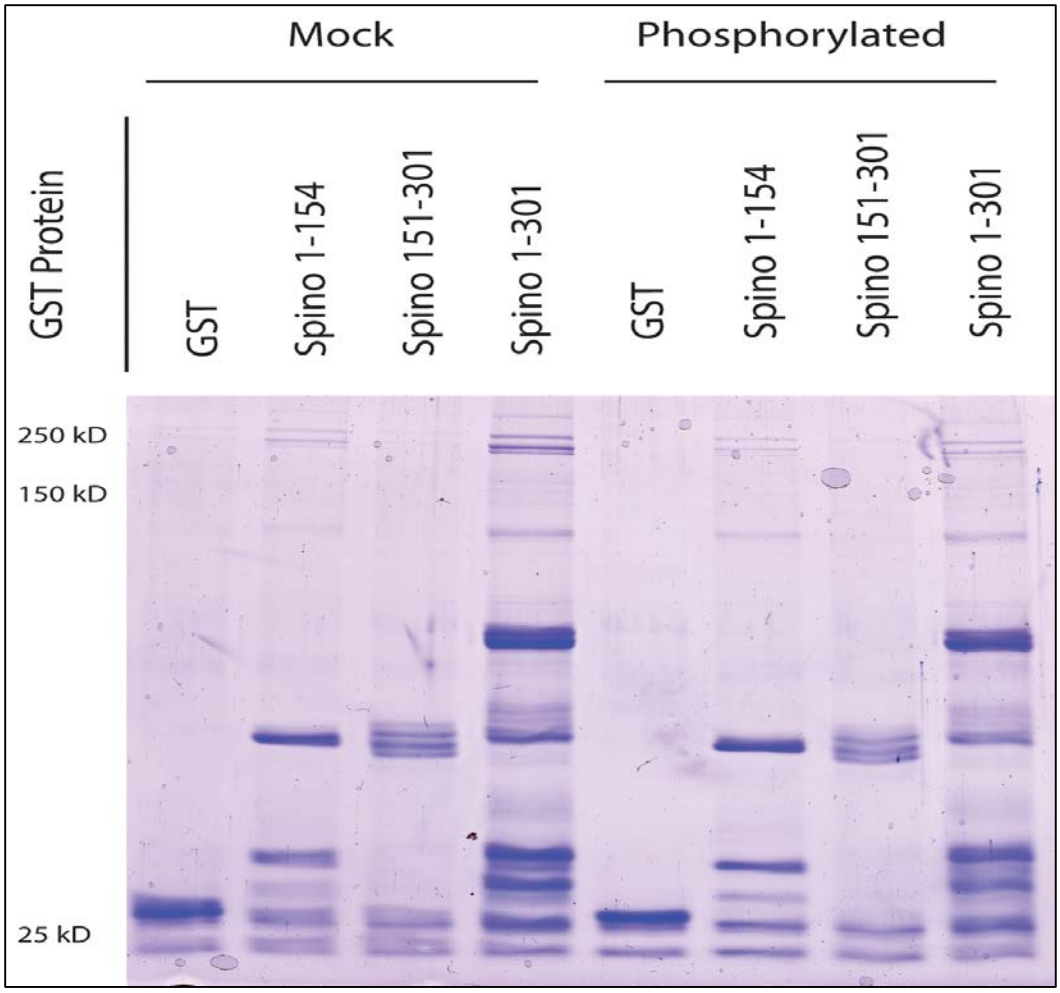

Figure 9: *In* vitro phosphorylation decreases spinophilin's association with various SpAPs. Spinophilin fragments were incubated with the catalytic subunit of PKA in the presence (phos.) or absence (mock phos.) of ATP. EDTA was added to each reaction mixture after incubation in order to halt catalytic activity. Mixtures were then incubated with mouse cortical lysate. GST pulldowns were performed and samples were submitted to SDS-PAGE before Imperial protein staining. Various band regions were excised and analyzed via MS/MS.

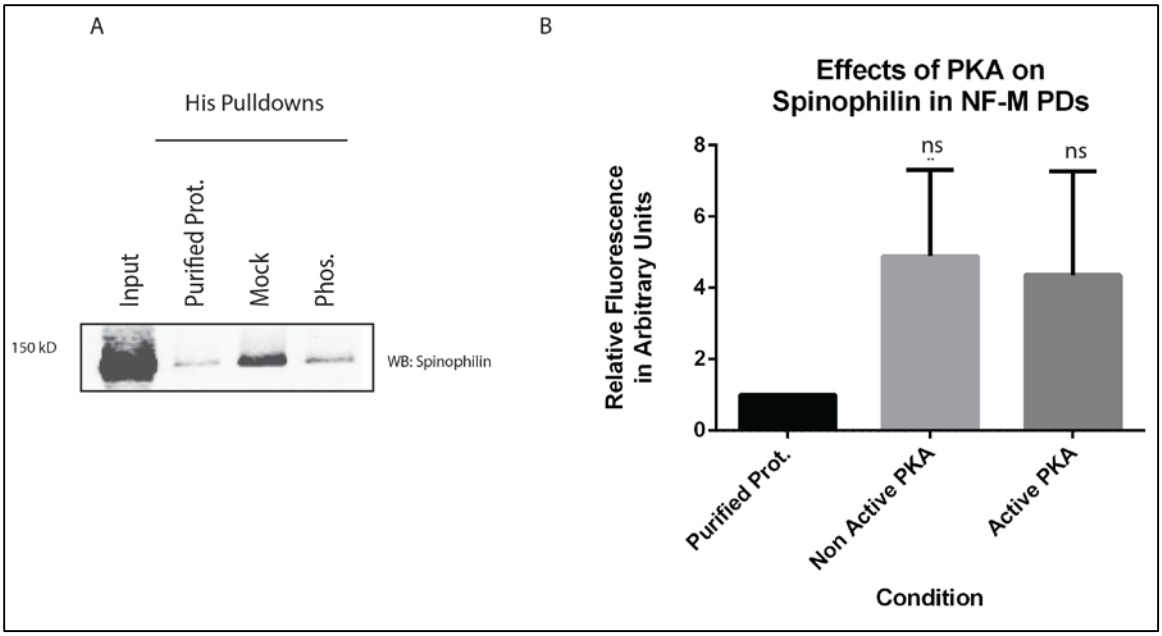

Figure 10: *In vitro* phosphorylation via PKA modulates the interaction between NF-M and spinophilin. A) NF-M was incubated with PKAc followed by mouse cortical lysate. His pull-downs were performed from lysate using Talon resin beads and samples were immunoblotted for spinophilin. **B)** Spinophilin fluorescence data were normalized back to the amount of NF-M in each sample. n = 4; p = 0.0672.

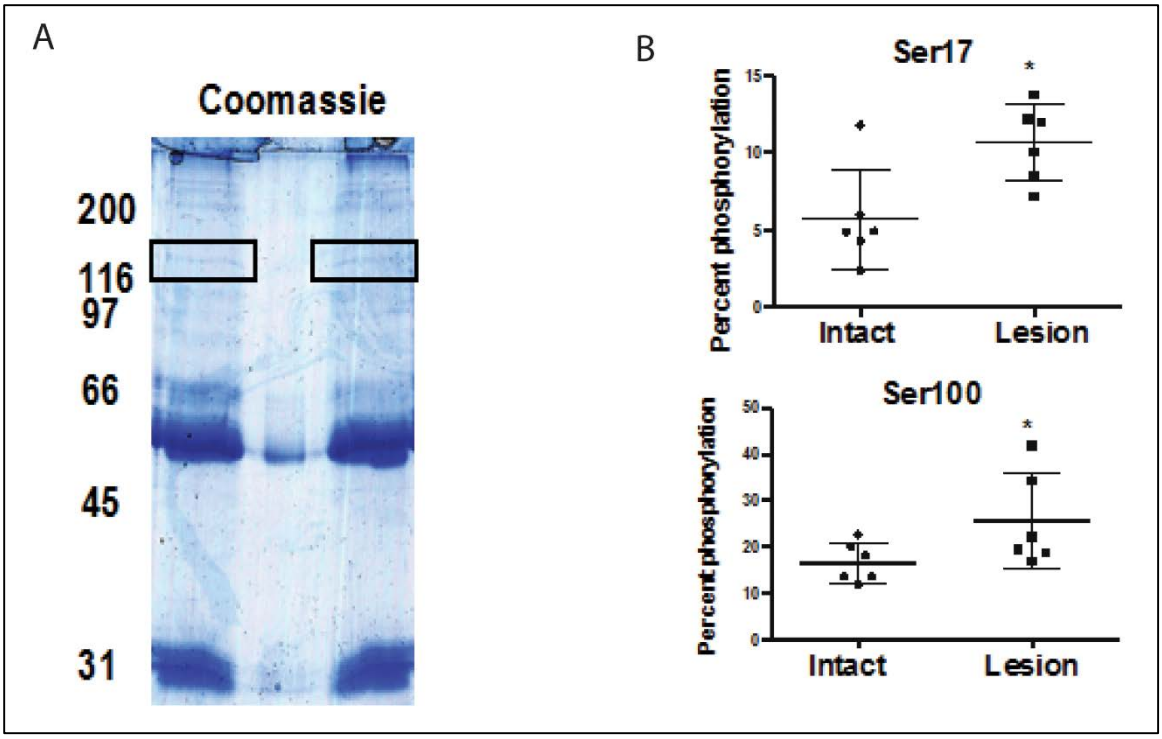

Figure 11: Phosphorylation at spinophilin Ser17 and Ser100 increases in an animal model of PD. A) Coomassie-stained gel showing bands that were excised for MS/MS analysis. **B)** Quantified data showing an increase in phosphorylation events in 6-OHDA lesioned tissue vs. intact tissue.

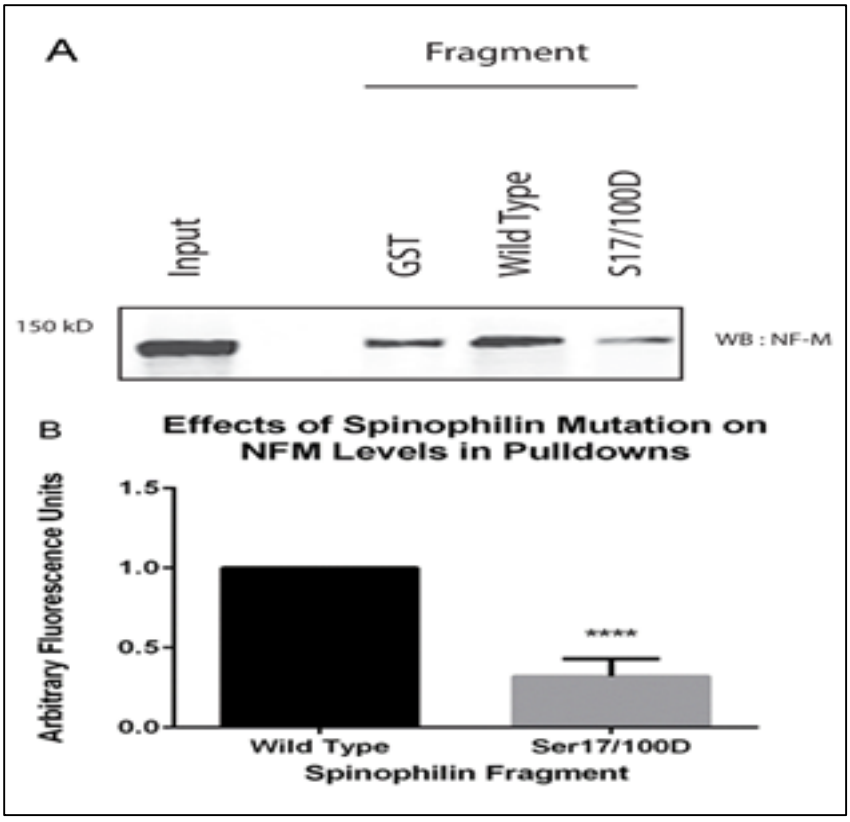

Figure 12: Mutating Ser17 and Ser100 to Asp attenuates the interaction between NF-M and spinophilin. A) Western blot obtained from GST pulldown experiment where mutant spinophilin fragments were incubated with cortical lysate. Immunoblotting was performed using antibodies for NF-M and GST. **B)** Quantified data in arbitrary fluorescence units showing a significant decrease in the level of NF-M in GST pulldowns when normalized to levels of GST-fused protein. $n = 4$; $p < 0.0001$.

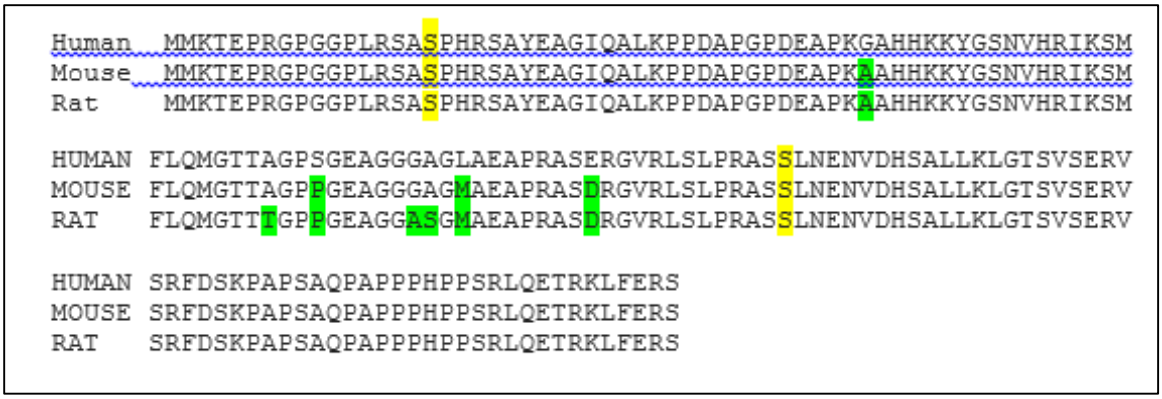

Figure 13: Spinophilin sequence alignment. Sequence alignment of the first 154 amino acids of spinophilin in human (Uniprot ID: Q96SB3), mouse (Uniprot ID: Q6R891), and rat (Uniprot ID: O35274). Ser17 and Ser100 are highlighted in yellow. Differences in protein sequences are highlighted in green (http://www.uniprot.org/align/).

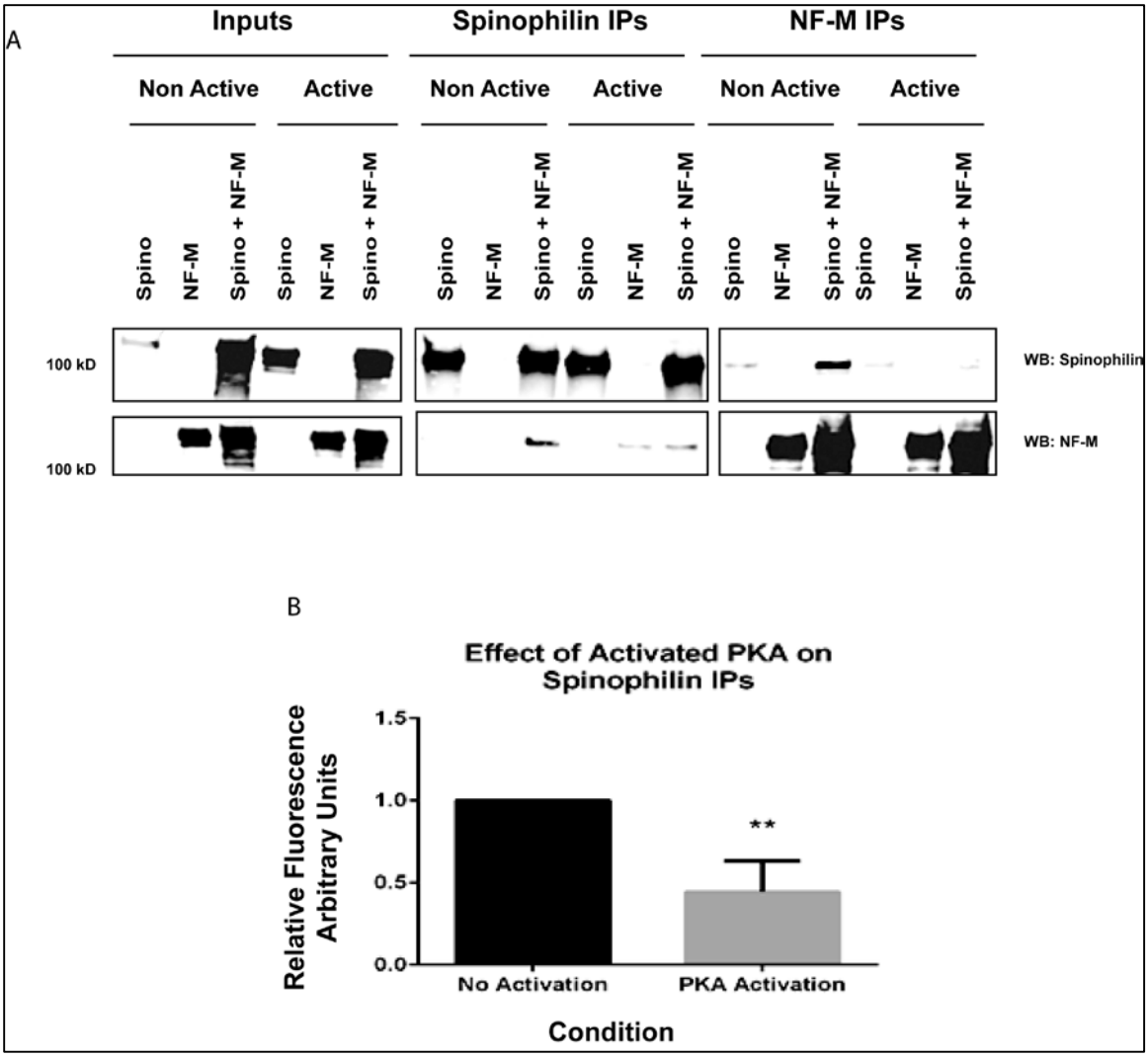

Figure 14: Short-term activation of endogenous PKA decreases the association of NF-M and spinophilin. A) Spinophilin and NF-M were transfected in HEK293 cells and PKA was endogenously activated. IPs were performed with antibodies directed against either the HA or V5 tag and immunoprecipitates were western blotted with antibodies directed against either spinophilin or NF-M. B) Quantified data show a decrease in the association between spinophilin and NF-M following PKA activation. $p < 0.05$. $n = 3$.

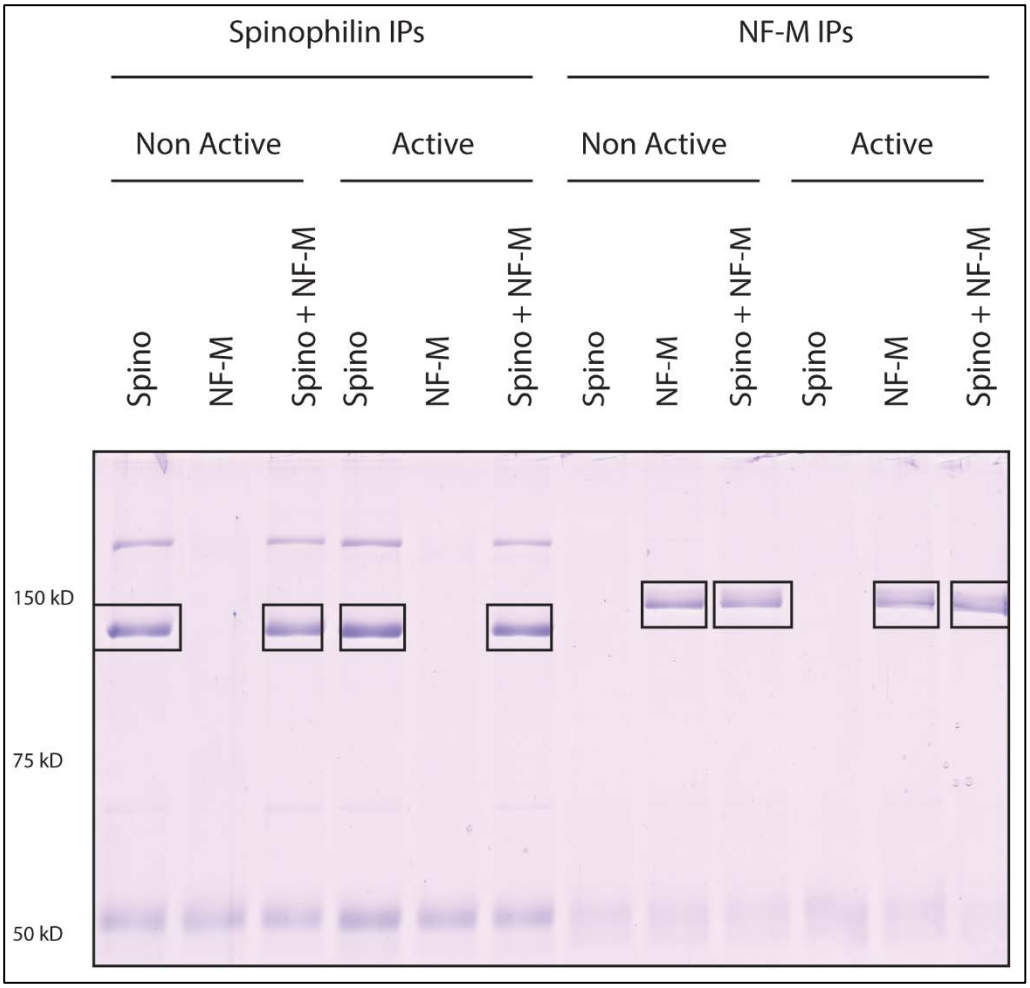

Figure 15: Short-term PKA activation Imperial stain. HEK 293 cells were transfected and endogenous PKA was activated as in Fig. 11. Samples were submitted to SDS-PAGE and Imperial stained. Outlined bands were excised and prepared for analysis via MS/MS.

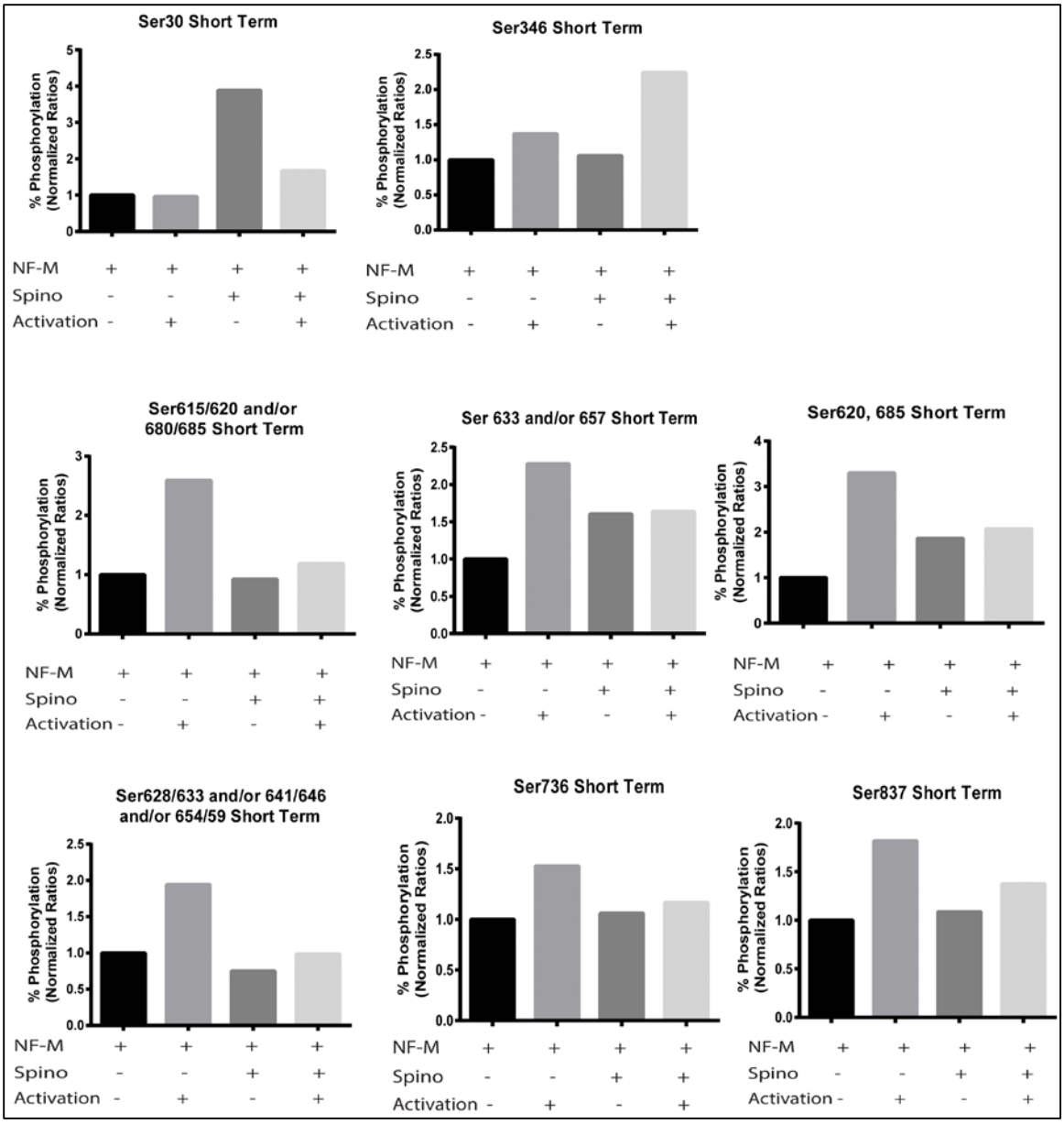

Figure 16: Phosphorylation levels of specific serines in NF-M after short-term activation. HEK293 cells were transfected with either NF-M, spinophilin, or both. Cells that were activated underwent a 30-minute incubation with IBMX and forskolin while non-activated samples were incubated with DMSO (vehicle). Samples were separated by SDS-PAGE and analyzed via MS/MS.

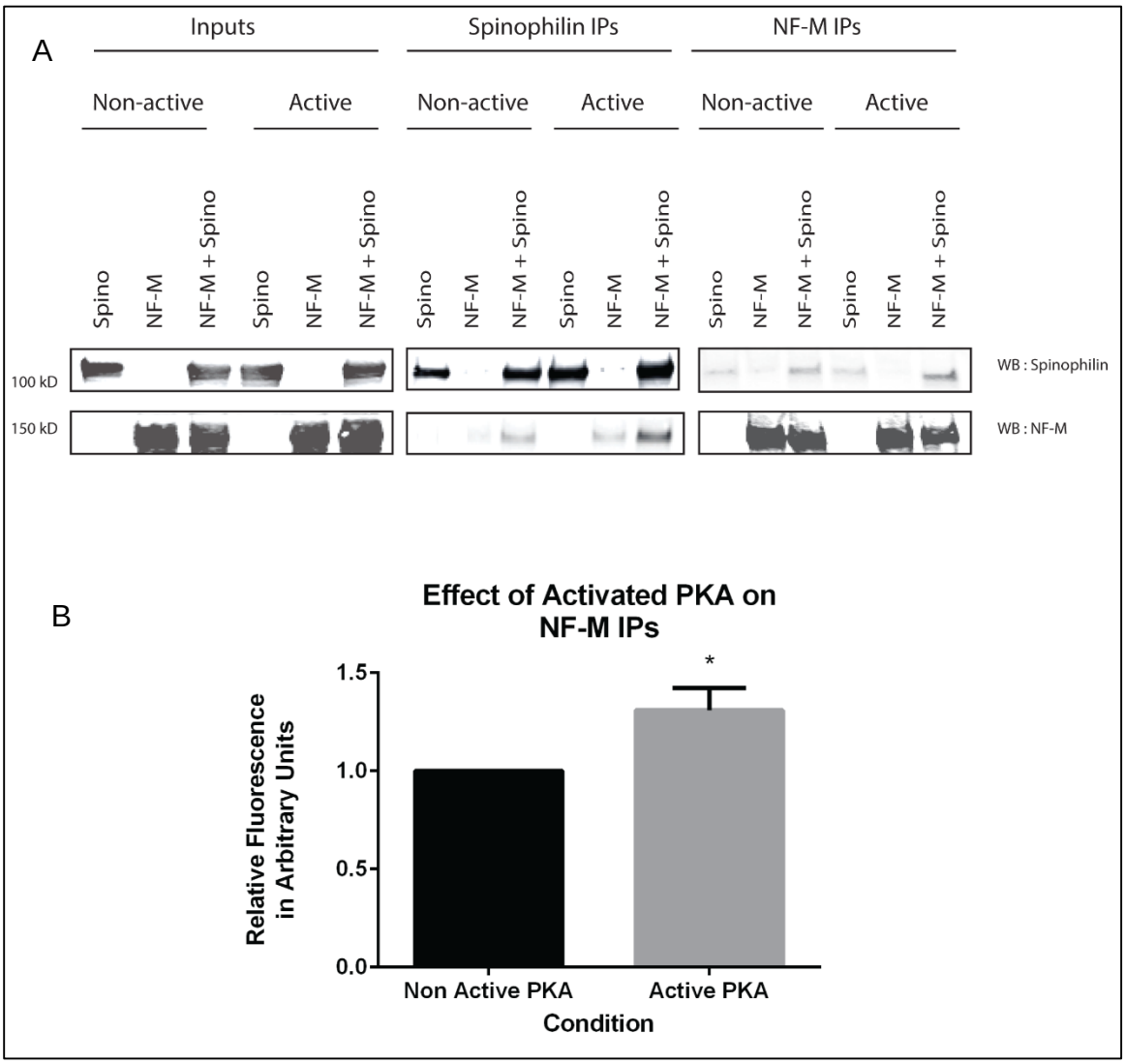

Figure 17: Long-term PKA activation increases the interaction between NF-M and spinophilin. A) NF-M and spinophilin were overexpressed in HEK293 cells. IBMX and forskolin were used to activate endogenous PKA over 16-20 hours. **B)** Quanitified data reveal increased levels of spinophilin in NF-M IPs when PKA has been activated. n = 4, p = 0.0123.

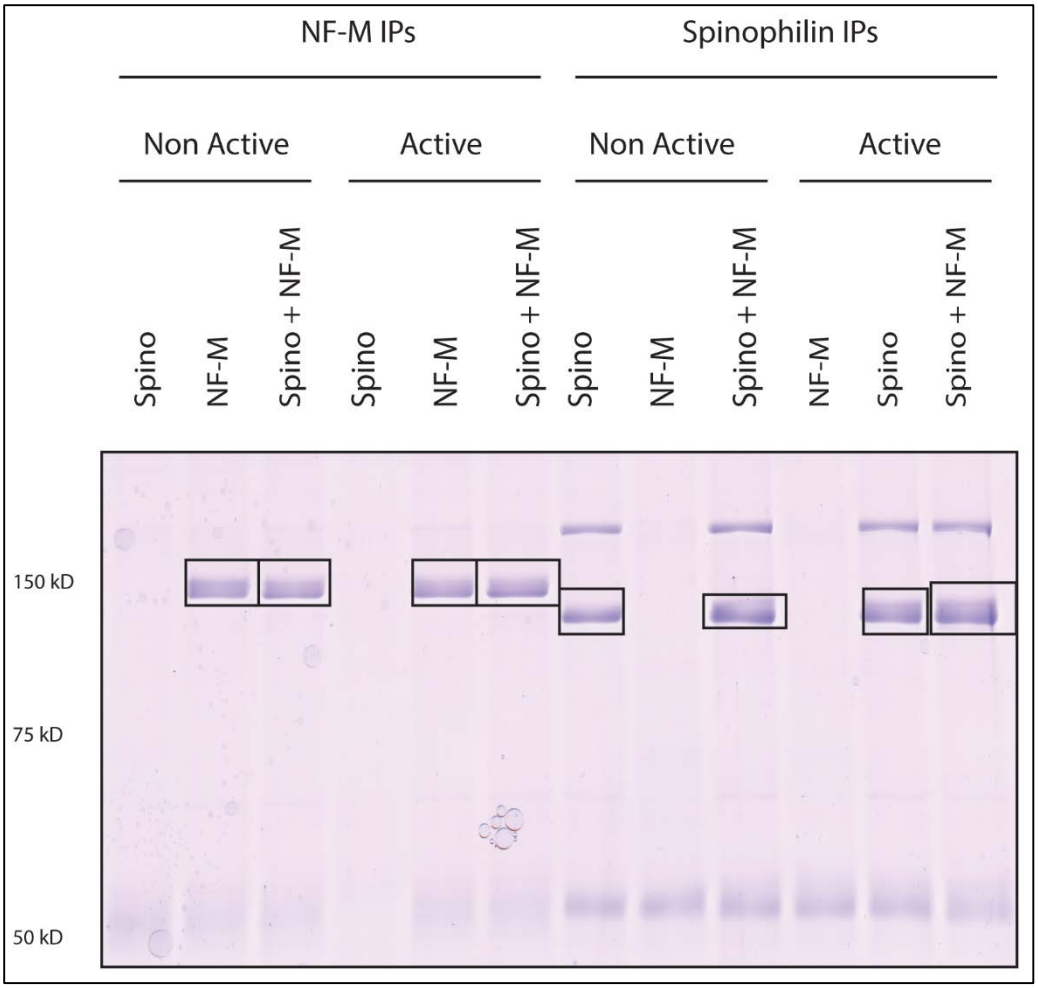

Figure 18: Long-term PKA activation Imperial stain. HEK 293 cells were transfected and endogenous PKA was activated as in Fig. 16. Samples were subjected to SDS-PAGE and Imperial stained. Outlined bands were excised and prepared for analysis via MS/MS.

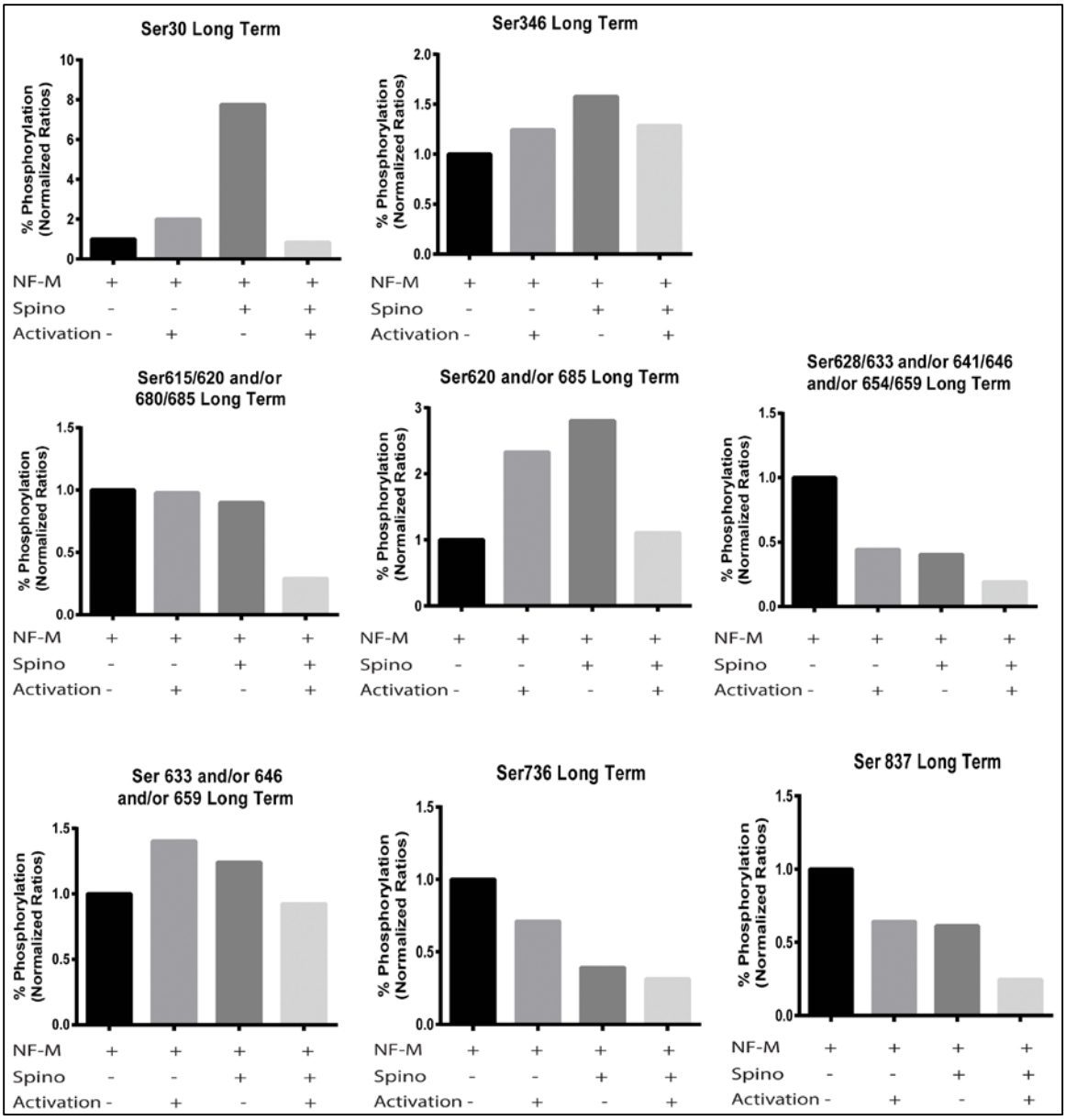

Figure 19: Phosphorylation levels of specific serines in NF-M after long-term activation. HEK293 cells were transfected with either NF-M, spinophilin, or both. Cells that were activated underwent a 16-20 hour incubation with IBMX and forskolin while non-activated samples were incubated with DMSO (vehicle). Samples were separated by SDS-PAGE and analyzed via MS/MS.

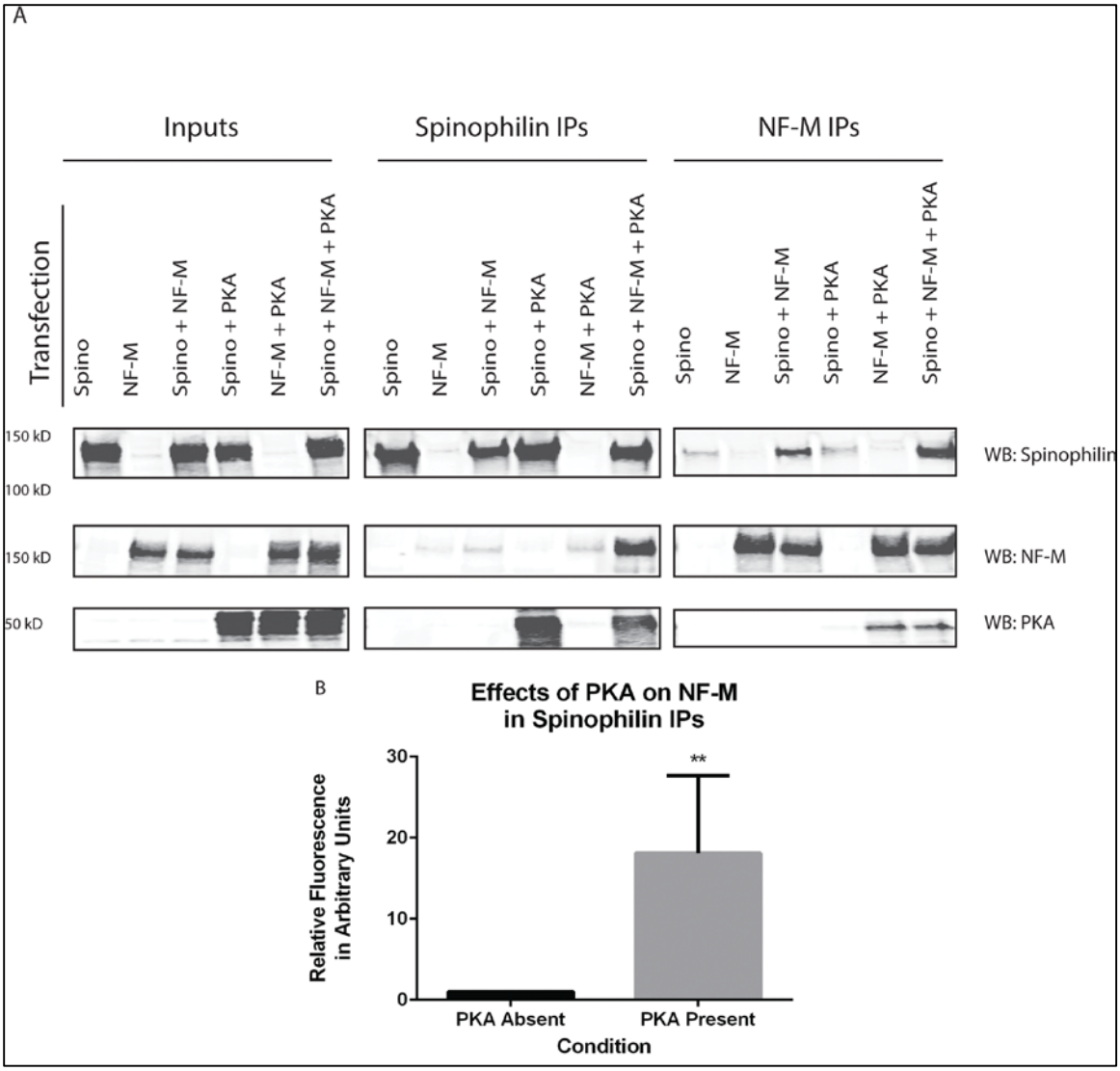

Figure 20: Overexpression of PKA in HEK293 cells enhances the association of NF-M and spinophilin. A) Western blot showing the increase in association between NF-M and spinophilin when PKA is overexpressed. Immunoprecipitations were conducted using antibodies for the HA (spinophilin) and V5 (NF-M) tags. Western blots were obtained using antibodies for spinophilin, NF-M, and PKA (top to bottom, respectively). **B)** Quantified immunoreactivity show a significant, ~20-fold, increased association between spinophilin and NF-M in the presence of PKA. $p = 0.004$, $n = 5$.

TABLES

Table 1. Spectral counts of specific neuronal proteins in wild type vs. knockout tissue when immunoprecipitated samples are analyzed via MS/MS.

	Goat IP	**Rabbit IP**
Protein	Spectra WT (KO)	Spectra WT (KO)
Neurofilament Light	4 (0)	19 (0)
Neurofilament Medium	2 (0)	8 (0)
α-internexin	5 (0)	14 (0)

Table 2. Spectral counts of spinophilin-associated proteins in samples where spinophilin fragment AA1-301 has been incubated with PKAc in the absence of ATP (mock) versus those incubated with PKAc in the presence of ATP (phosphorylated.

Protein	**Mock**	**Phosphorylated**
Myosin-10	224	40
Myosin-Va	188	22
Spectrin	79	41
Myosin-14	29	3
NF-M	5	2
NF-H	5	0